Medium-scale experiments on DeNo/DeSO_2 from flue gas by pulsed corona discharge

tu/e
Research Report
ISSN 0167-9708
Coden: TEUEDE

Eindhoven
University of Technology
Netherlands

Faculty of Electrical Engineering

Medium-scale Experiments on DeNO/DeSO2 from Flue Gas by Pulsed Corona Discharge

by
L.M. Zhou
E.M. van Veldhuizen

EUT Report 96-E-302
ISBN 90-6144-302-4
December 1996

Eindhoven University of Technology Research Reports

Eindhoven University of Technology

Faculty of Electrical Engineering
Eindhoven, The Netherlands

ISSN 0167-9708 Coden: TEUEDE

Medium-scale Experiments on DeNO/DeSO2 from Flue Gas by Pulsed Corona Discharge

by

L.M. Zhou
E.M. van Veldhuizen

EUT Report 96-E-302
ISBN 90-6144-302-4

Eindhoven
December 1996

CIP-DATA LIBRARY TECHNISCHE UNIVERSITEIT EINDHOVEN

Zhou, L.M.

Medium-scale experiments on DeNO/DeSO2 from flue gas by pulsed corona discharge / by L.M. Zhou and E.M. van Veldhuizen. - Eindhoven : Eindhoven University of Technology, 1996. -VI, 34 p.
(Eindhoven University of Technology research reports ; 96-E-302). - ISBN 90-6144-302-4
NUGI 832
Trefw.: ontzwavelen / stikstofoxiden / coronas / elektrische gasontladingen / rookgassen / hoogspanningspulsen.
Subject headings: flue gas desulphurisation / corona / electric discharges / pulsed power technology.

Medium-scale experiments on DeNO/DeSO$_2$ from flue gas by pulsed corona discharge

Zhou L.M. and E.M. van Veldhuizen

Abstract

Pilot-scale experiments on the simultaneous removal of SO_2 and NO_x from flue gases have been conducted. UV absorption to simultaneously detect NO (0-450 ppm), SO_2 (0-1000 ppm) and NH_3 (0-1000 ppm) is applied to the flue gas cleaning process using pulsed corona discharge. The measurement error is in all cases below 5% despite of spectral overlap. The good agreement on the removal effects with results from literature shows that this is a viable method. Flue gases produced using a methane burner are treated in a pulsed corona reactor with 6-80 Nm^3/h flow. The initial concentrations of SO_2 and NO are about 300 ppm in flue gas. The pulses of voltage with about 100 ns rising time and 180 ns half-width are used to produce the pulsed streamer discharges. The results show that the energy cost of the removal of NO and NO_x can be reduced through optimizing the energization and gas conditions including dc bias, temperature, residence time, synergetic effect of NO, SO_2 and NH_3. The auto-thermal reaction of SO_2-NH_3 is dominant for SO_2 removal. The increase in input of discharge energy has only a small influence on the SO_2 removal, but the slip of NH_3 can be reduced to almost zero by increasing the power input. It is observed that the removal rate of SO_2 depends to a great extent on the time sequence of experiments. This strong history effect is beneficial for SO_2 removal with corona discharge and NH_3 injection. NH_3 injection enhances the NO removal but its slip is high. SO_2 presence in flue gas enhances NO removal also, in combination with NH_3, however, the enhancement becomes less than either of them. Through adjusting locations of SO_2 or NH_3 injection, synergetic effects on NO removal can be greatly enhanced. With an optimum residence time of about 15 s and the use of history and synergetic effects, more than 95% SO_2 and 85% NO are removed with 3 ppm leak NH_3, resulting in a energy cost of 13 eV/NO. With shorter pulses, further improvement of NO removal is still expected to be possible.

Keywords: flue gas, SO_2/NO_x removal, pulsed corona discharge, UV absorption, synergetic effect

- Zhou L.M. and E.M. van Veldhuizen
  Medium-scale experiments on DeNO$_x$ /DeSO$_2$ from flue gas by pulsed corona discharge.
  Eindhoven: Faculty of Electrical Engineering, Eindhoven University of Technology, 1996.
  EUT Report 96-E-302
- Adresses of the authors:
  Zhou Li-Ming
  Division of High Voltage, School of Electrical Engieering, Xi´an Jiaotong University
  Xi´an 710049, P.R. China

  E.M. van Veldhuizen
  Division of Electrical Energy Systems
  Faculty of Electrical Engineering
  Eindhoven University of Technology
  PO Box 513, 5600 MB Eindhoven, The Netherlands

Preface

This report is a summery of the experimental work at Eindhoven University of technology from December 14, 1995 to September 1, 1996. During this period, I was on leave from the Xi'an Jiaotong University and worked at the Eindhoven University as a postdoctoral fellow under the guidance of Dr. E.M. van Veldhuizen. My stay in Eindhoven is financially supported by EUT as a part of EUT-XJTU exchange programme.

My first thanks are given to Dr. E.M. van Veldhuizen for his guidance at each step of this research work. I wish to thank Prof. W.R. Rutgers for stimulating discussions and invaluable suggestions. I like to give my true thanks to Loek Bade for the close co-operation and always help during the experiments. I also like to give my thanks to Ad Holten and Wilfred Hoeben for their particular help on the computer. I like to thank my wife, Li Lin, who joined me from USA and supported me to complete this investigation.

Final thanks are ascribed to the Eindhoven University of Technology for the provision of a research scholarship.

Zhou Li-Ming

August , 1996

CONTENTS

	page
1. Introduction	1
1.1 General	1
1.2 Current status	1
1.3 Present objectives	1
2. Discription of experimental system	3
2.1 Flue gas cleaning set-up	3
2.2 Pulse power supply	4
2.3 UV absorption set-up	6
3. UV absorption measurements	6
3.1 Absorption spectra	6
3.2 Calibrations	9
4. Cleaning measurements	11
4.1 Removal of NO/NO_x	11
4.1.1 DC bias effect	11
4.1.2 Residence time effect	13
4.1.3 O_2 and H_2O effect	14
4.1.4 Temperature effect	15
4.2 Removal of SO_2	16
4.2.1 Removal of SO_2 in air	16
4.2.2 Removal of SO_2 in flue gas	17
4.2.3 History effect	18
4.3. Combined removal of NO and SO_2	18
4.3.1 SO_2 effect on $DeNO/DeNO_x$	18
4.3.2 Synergetic effect of SO_2, NO and NH_3	19
4.3.3 NH_3 effect on the removal of SO_2 and NO	20
4.3..4 Enhancement of synergetic effect	20
5. Two-stage cleaning measurements	22
5.1 NO and NO_x removal	22
5.2 Combined removal of SO_2 and NO	23
6. Removal of NH_3	24
7. Discussion	24
8. Conclusions	28
9. References	30

1. Introduction

1.1 General

NO_x and SO_2 emissions are the main cause of the acid rain. A increasing public and official concern calls for powerful treatment. To meet this requirement, combined removal of NO_x and SO_2 (generally referred to as combined $DeNO_x/DeSO_2$ from the flue gas by pulsed corona discharge has been comprehensively investigated in the past decade. The possibility of an application of pulsed corona discharges to simultaneous removal of SO_2 and NO_x from the flue gas of coal-fired power stations has been experimentally confirmed at ENEL [1]. Based on ENEL experimental results and compared with other processes (Calcium-Gypsum + Ammonia Catalytic, E-Beam), the pulsed corona method has presented the most economical means for the next generation $DeNO_x/DeSO_2$ [2]. The general advantages of pulsed discharge technology for industrial application are suggested as: (1) it simultaneously removes NO_x and SO_2 in a single dry process; (2) it could be retrofitted in existing electrostatic precipitation; (3) it requires a low ground surface; (4) its by-product is dry powder which could be easily collected by an electrostatic precipitator; (5) the by-product could be directly used as an agricultural fertiliser.

1.2 Current status

During the $DeNO_x/De/SO_2$ process with pulsed corona discharge in combination with ammonia injection, the pulsed corona induced chemical reactions are generally divided as essential radical initiated reactions and spontaneous reactions. For the removal of SO_2, auto-thermal reactions of SO_2-NH_3 are supposed to play the most important role. In contrast, the NO_x molecules are mainly oxidized by radical reactions. Comparatively, the removal of NO_x is energy cost and its chemistry is also much more complex. Take ENEL experimental results as a typical example, 99 % SO_2 can be easily removed with corona discharge and NH_3 and H_2O_2 injection [3]. But, the corona discharges alone can only convert about 10 % SO_2 in most cases. NO_x removal mainly depends on the energy input of discharges. For this reason, the removal rate (%) and energy costs per removed NO_x molecule (eV/NO_x) from flue gas in the literature are generally used to evaluate the cleaning efficiency. At ENEL, 50-60 % of 250-500 ppm NO_x is removed at the energy input of 12-15 Wh/Nm^3, corresponding to a minimum energy cost of 50 eV/NO_x [1]. It is estimated to be 5-6 % of power plant output. Such an energy requirement is still too high for commercial application. However, one should bear in mind that experiments up to now have been performed with a rather limited set of conditions mainly in an empirical way and small scale. The whole process is not fully optimized yet and the chemistry of the process is only superficially understood. Before this technology is put into practical application, it is essential to scale up the treatment process for obtaining a better understanding of the SO_2/NO_x conversion mechanism and finding the best technical approaches. Under this circumstance, systematic experiments are conducted to reveal the importance of experimental conditions. In the first stage, the pilot-scale experiments have confirmed the importance of optimization of gas conditions and energization parameters for improving the energy efficiency: without any additive the energy cost of 20 eV/NO has be obtained using voltage pulses with about 20 ns and a 60-70 °C flue gas with a residence time of 15 s [4]. Although only a part of the parameters has been optimized in these experiments, they have already indicated that, with optimizing conditions, the energy cost can be lowered to satisfy a energy requirement of 1-2 % (less than 20 eV/NO) of the output of the power plant.

1.3 Present objectives

The general objective of the investigation is to lower the energy cost at required removal rates of NO_x and SO_2 in real flue gas. Regarding the amount of NH_3 injection, both improvements of SO_2 and NO_x removal rates and the reduction of NH_3 slip (<5 ppm, in The Netherlands) will be taken into

account in the investigations. The present work at EUT, in general, consists of two subjects:

(1) Detection of SO_2, NO and NH_3 by UV absorption

As the first and essential step, UV absorption is developed to detect on-line and simultaneously NO, SO_2 and NH_3 in the cleaning process in order to avoid the interference of NH_3 injection on the previously used gas analyzer. The part of the results on this subject has been reported in [5] .

(2) Cleaning measurements on removal of SO_2 and NO_x

For the removal of NO/NO_x, the main attention will be paid to finding the optimum energization conditions including gas conditions and electrical parameters such as gas temperature, gas flow rate or residence time, dc bias level, NH_3 injection.

For the removal of SO_2, the auto-thermal reaction of SO_2-NH_3, corona discharge and both in combination are systematically investigated. The gas temperature and water content in the flue gas will be the main parameters in question.

For combined removal of SO_2 and NO with and without NH_3 injection, the synergetic effects between SO_2, NO and NH_3 will be mainly focused on. Positive effects are expected to lower the energy cost of the removal of NO_x.

Since some parameters, including pulse risetime and gas temperture, have been known the best values for the removal of NO at EUT [4], the present work is based on these previous investigations and to futher optimize the cleaning process in flue gases with about 300 ppm NO and 300 ppm SO_2. The part of the results on this subject has also been presented in [6].

2. Description of experimental system

2.1 Flue gas cleaning set-up

An overview of the complete set-up at EUT is given in the figure 1. This pilot-scale system uses a methane burner with a maximum output of 300 Nm^3/h [7]. The flue gas partly goes through a wire-cylinder corona reactor, which consists of two chambers in series with a length of 2.88 m and 2.77 m, respectively. The diameter of corona wire is 3 mm and the cylinder inner diameter is 0.2 m.

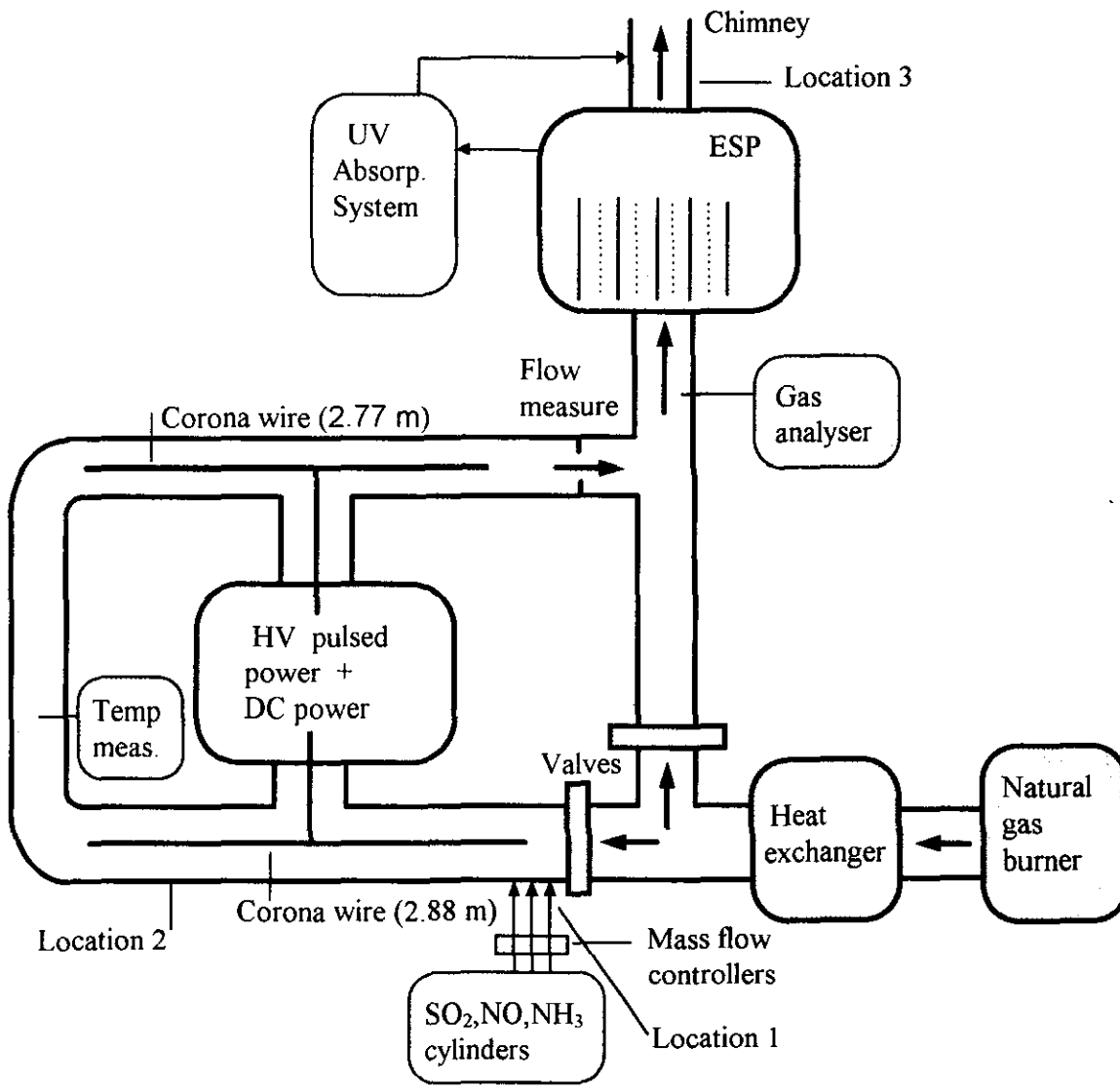

Figure 1: An overview of the complete pilot-scale set-up for flue gas cleaning at EUT

The reactor can be used to perform the single-stage (with 2.88 m chamber) and double-stage (with two chambers in series) flue gas treatment experiments. Although the parameters of electrodes such as the diameter of corona wire and the gap spacing are important for the optimisation, they are temporarily fixed in this work. The gas temperature in the reactor can be adjusted between 60 and 130 °C by the aid of the electrical heating and gas flow. The flue gas flow can be varied from 6 to 80 Nm^3/h. The total gas flow through the corona section is measured with a pressure difference flange with 2 % accuracy. The typical flue gas from the burner has a composition of 6 % O_2, 8 % CO_2, 16 % H_2O and 70 % N_2. In this report, the flue gas with such a composition is referred to as "standard flue gas" from here on. The O_2 and CO_2 contents in flue gas flow are measured with a electrochemical analyser (SONOX Rend-O-meter) which is calibrated before the systematic measurements. The H_2O content is estimated as two times content of CO_2 assuming that pure methane is burned. To observe the influence of gas composition on the removal of SO_2 and NO_x, the O_2, CO_2 and H_2O contents in flue gas can be varied by adding excess air. In this system, a increase of O_2 content naturally causes a decrease of CO_2 content. The change of total gas flow through the reactor also causes a change of gas temperature. The pollutant gases of NO, SO_2 and NH_3 gases are introduced from gas cylinders through calibrated mass flow controllers. Before the measurements, the mass flow controllers are calibrated with gas analyser for NO in flue gas and for SO_2 in air. Afterwards, the mass flow controller for NH_3 is calibrated with the thermal-reaction of SO_2-NH_3 in room air. In the calibration of gas flow controller of NH_3, much high concentration of SO_2 is used. The amount of the injected NH_3 is calculated as two times the concentration of removed SO_2 when no slip of NH_3 can be see from the UV absorption spectra. We believe that this method is valid because the NH_3 absorption is easily seen from the UV spectra at 213.4 nm or 204 nm. The accuracy of NH_3 flow controller is estimated as the sum of the accuracy of SO_2 (3 %) and total flow measurement (2 %). In this way, the system error for gas detection can be reduced to a minimum. With flow controllers, NO and SO_2 are usually injected with an initial concentration of about 300 ppm (with 10 ppm maximum deviation) and in most cases the amount of NH_3 injection is less than its stoichiometric value of 900 ppm (with 45 ppm deviation or less). A flue gas composition like this is realistic for a power plant combusting low-sulphur coal. In our cleaning process with NH_3 injection, SO_2, NO and NH_3 are detected by UV absorption at the exit of the system. In the absence of NH_3 injection, SO_2 and NO_x (i.e. NO+NO_2) and NO are detected using an electrochemical analyser.

2.2 Pulse power supply

The electrical pulses used in the experiments are created with a triggered spark gap switched capacitor, see figure 2. Two examples of voltage and current waveshapes are given in Fig.3. With the aid of HV transformer, upto 70 kV voltage pulse can be output with a rise time of about 100 ns and a half-width of 180 ns. Due to the large inductance of the transformer, the maximum pulse voltage rise rate is about 0.7 kV/ns and the tail of the voltage pulse has a long and decayed oscillation. The half-width of corona current pulse is 140-150 ns. This is almost four times higher than the streamer transition time of 30-40 ns [4]. One should bear in mind that the parameters of pulses used here are not the optimum values for this electrode system [4]. A dc bias voltage upto 30 kV can be added to corona wire which leads to higher current pulses and higher input discharge energy. The supply can be operated up to 250 Hz. The electrical energy input into the corona discharge is usually varied by changing of the pulse frequency. The pulse voltage is measured with a capacitive-resistive divider (Tek. P6015) with a division ratio 1/1000. The current pulse is measured with a Rogowsiki coil (Pearson model 2877, inner diameter 6 mm, rise time 2 ns). Both the voltage and current pulses are detected with a digital oscilloscope with 300 MHz analogue bandwidth and 2 ns sample time (Tek.DSA 601). Data are transmitted from the oscilloscope to a

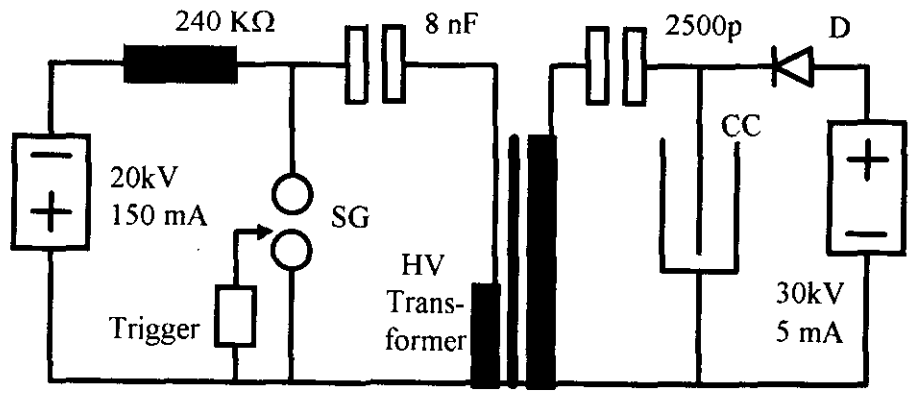

Figure 2: The electrical circuit for the production of HV pulses with a dc bias.

computer via a GPIB interface. The total power per pulse can be calculated by multiplying the current and voltage waveforms. The associated discharge energy is obtained by the interruption of the power and the subtracting the capacitive energy of the electrode arrangement. The measurements of the electrical energy input with high time resolution have been described in more detail elsewhere[8]. The energy cost W_m (in unit of eV/molecule) of the cleaning process is calculated from the specific discharge energy E (in unit of Wh/Nm^3) and the amount of removed molecules DeN (in unit of ppm):

$$W_m = 897\ E\ /\ DeN$$

Figure 3: Two examples of voltage and current waveshapes.

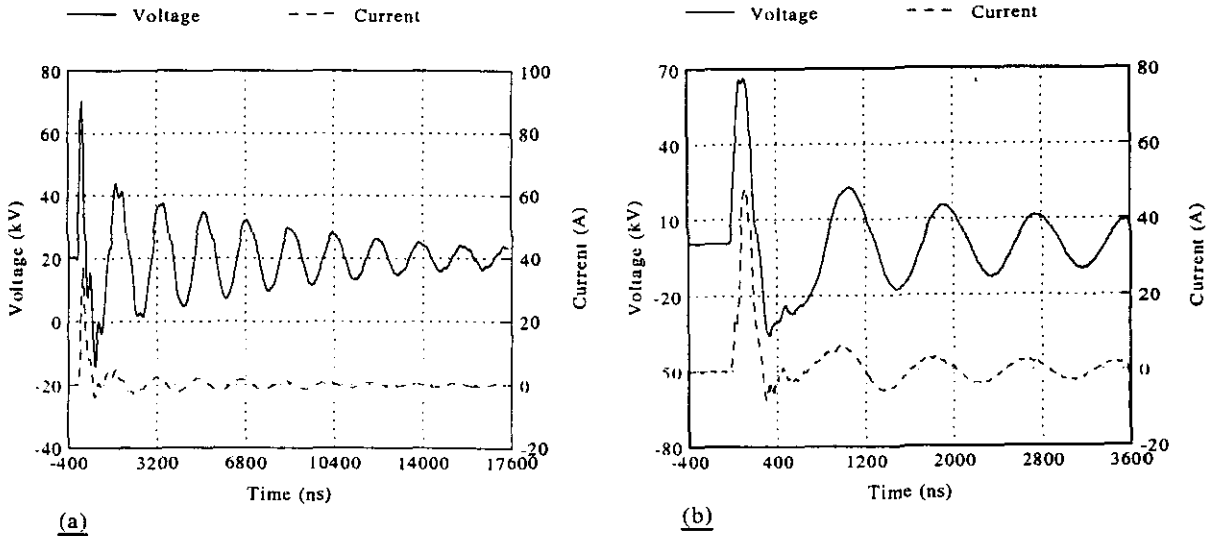

(a) V_{dc}=20 kV, V_p=70 kV, f=100 Hz; Per single pulse: Q_{tot}=9567 nC, Q_{cro}=9438 nC (98.6%), E_{tot}=510 mJ, E_{cro}=507 mJ(99%). (b) V_{dc}=0.0 kV, V_p=66 kV, f=50 Hz; Per single pulse: Q_{tot}=6318 nC, Q_{cro}=5869 nC (95%), E_{tot}=412 mJ, E_{cro}=410 mJ (99.6%).

2.3 UV absorption set-up

A UV absorption system is located at the exit of the cleaning set-up for the gas detection (fig.1). Figure 4 is the diagram of UV absorption system. The light source used in this system is a high pressure Xe lamp with 0.5 J input energy per pulse. With a lens with a focal length of 20cm in front of the lamp a parallel light beam is produced.

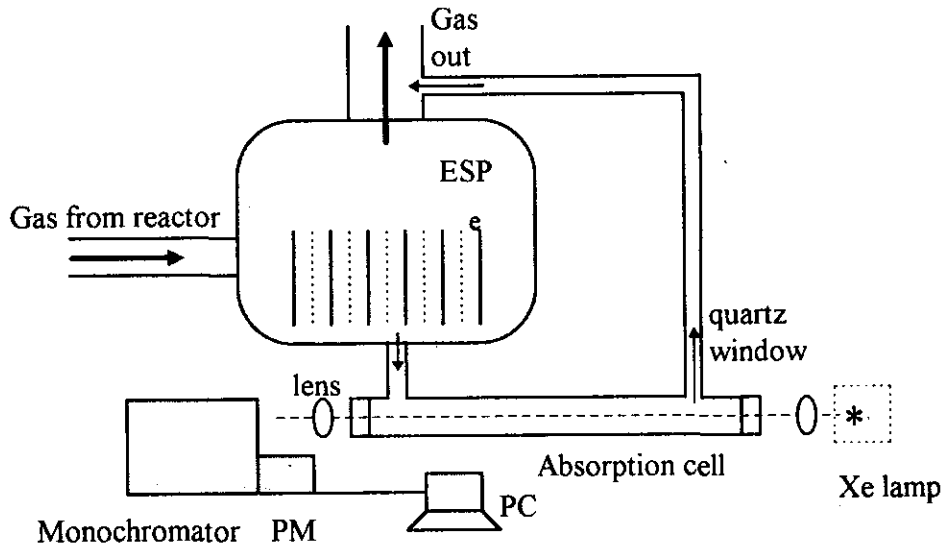

Figure 4: Schematic diagram of UV absorption system.
(The length of cell:1.53 m, Temp. in cell: over 100 °C.)

After passing through the gas absorption cell of 1.53 m in length, the light is focused with the second lens (f= 20 cm) onto the entrance slit of a 0.5 m Jarrel Ash monochromator (slit width: 50 mm). The light is detected at the output slit with a Hamamatsu R666 Photomultiplier (PM) with GaAs cathode. The PM is operated at -830 V in the scan of 200-237.5 nm and -600 V in the scan of 280-320 nm, respectively. The electrical signal (0-2V) from the PM is digitised by a 12-bit analogue-to-digital converter and read out by a microcomputer. A spectral scan of 200-237.5 nm takes 3 mins and yields 3276 points. The collected data is analysed using the well-known modified Beer-Lambert law:

$$I(l)=I_0(\lambda)\exp(\sigma(\lambda)CL)$$

where I_0 and I are the light intensities with and without absorption, while $\sigma(\lambda)$ denotes the absorption cross section of a gas at wavelength λ, C the concentration of measured gas and L the optical path length of the absorption cell. I_0 is calculated at wavelength λ using linear curve-fitting.

3. UV absorption measurements

3.1 Absorption spectra

SO_2, NO and NH_3 have several strong absorption bands in the ultraviolet region of the spectrum. These features in principal can be exploited to measure gas concentrations in flue gas cleaning process. But we have observed that a variety of factors influences absorption measurements, including:

(1) the presence of mist, water vapour and particles in the path cause light absorption and light

scattering which give rise to a complex, unstable absorption spectrum and therefore to cause difficult to accurately measure I_0;

(2) the cross sections for NO and NH_3 are concentration-dependent(see calibrations);

(3) the saturation of the absorption bands with increasing concentration;

(4) a gas mixture with SO_2, NO and NH_3 leads to overlap of absorption bands;

In order to avoid the particles and aerosol enterring into absorption cell, an electrostatic precipitator is installed before the absorption cell. The absorption cell is heated over 100°C to avoid the occurance of water condensation.

Figure 5: NO absorption spectra in 80° C flue gas flow.

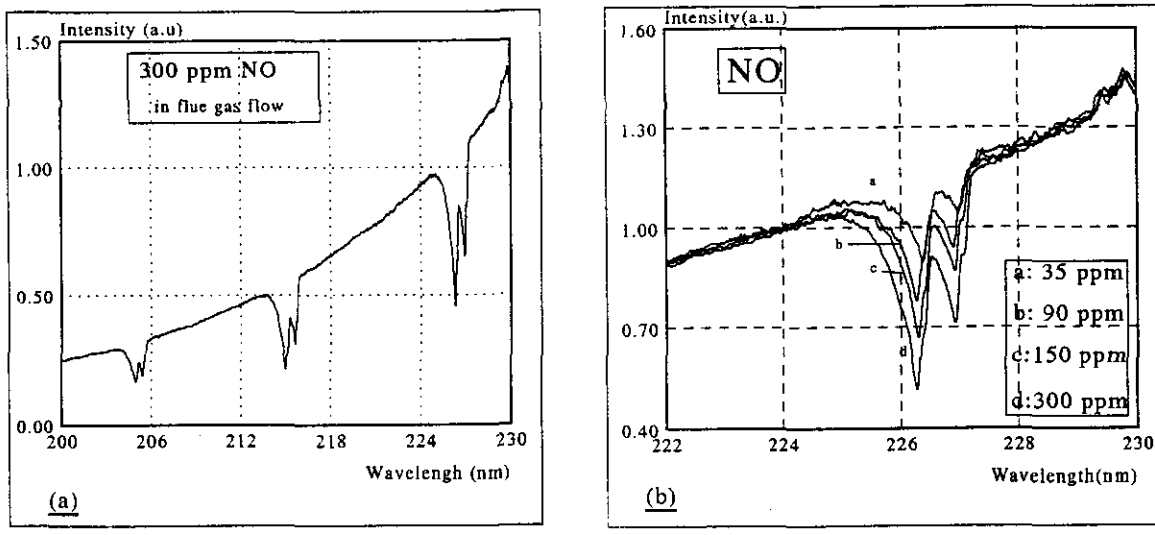

(a)In the region of 200-230 nm NO presents three strong absorption bands at 205 nm, 214.5 nm and 226.2nm. (b) UV absorption at 226.2 nm using four values for the concentration of NO.

Figure 6: SO_2 spectrum in 65° C air flow.

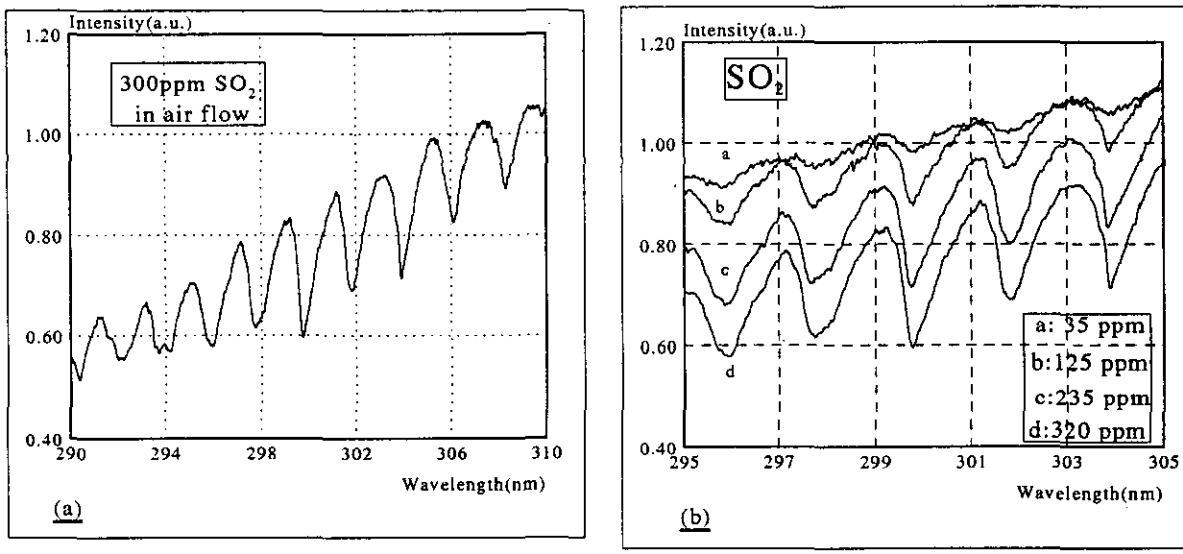

(a) Fine structure at 290-310 nm. (b) The absorption near 300 nm for four values of SO_2 concentration.

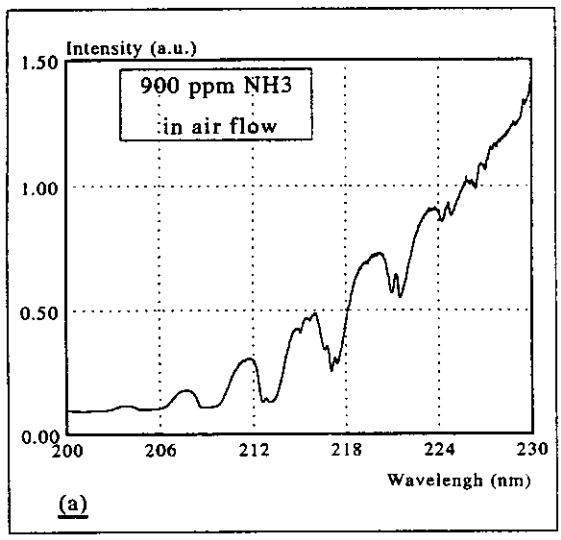

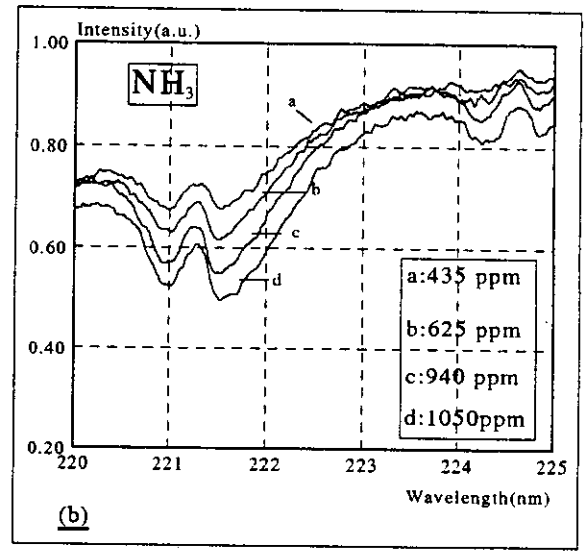

Figure 7: NH_3 spectrum in 70° C air flow with intentional injection of 10 ppm NO.

(a)in the region of 200-230 nm, absorption maximum at around 204nm, 209nm, 213nm, 217nm and 222 nm.

(b)NH_3 absorption spectra at around 213.4 nm for 0-435 ppm.

(c)NH_3 absorption spectrum at around 221.6 nm for 435-1050 ppm.

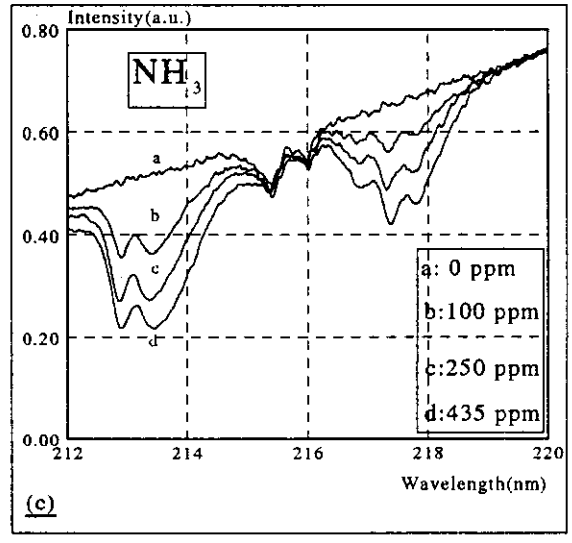

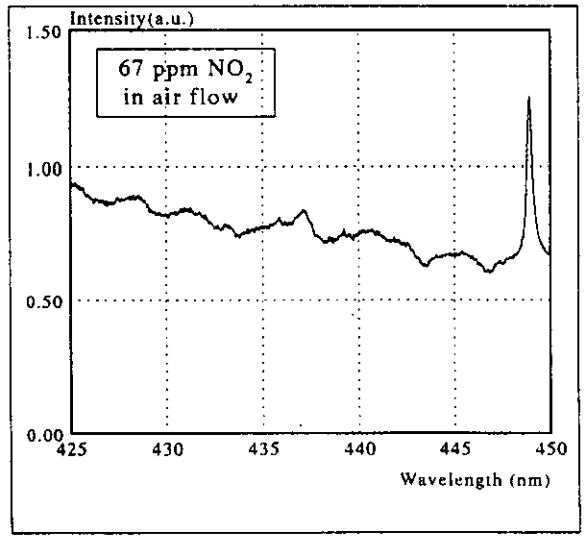

Figure 8: 67 ppm NO_2 absorption spectra in the region of 425-450 nm in 80 ° C air flow with corona discharge. It's too weak to be detected with reasonable accuracy.

In the region of 200-230 nm NO presents three strong absorption bands at 205 nm, 214.5 nm and 226.2nm as shown in figure 5(a). In fig.5(b), the NO absorption of (0,0) gamma-band located at 226.2 nm is shown using four values for the concentration of NO. With increasing concentration of NO, it is observed that absorption at 205 and 214.5 nm are readily saturated as compared with that at 226.2 nm. In order to obtain a high measurement accuracy in the range of 0-450 ppm, absorption band at 226.2 nm is employed for NO detection. SO_2 presents a very broad spectrum with a fine structure in 290-310 nm, as shown in fig.6(a). The absorption maximum around 300 nm is used for SO_2 detection. The absorption around 300 nm are shown in fig.6(b) for four values of SO_2 concentration. The leak NH_3 at the exit of the system is specially included in our measurements. The ammonia spectrum in the region of 200-230 nm exhibits absorption maxima at around 204nm, 209nm, 213nm , 217nm and 222 nm as shown in fig.7(a). Fig.7(b) and (c) give the NH_3 absorption spectra in the room air flow at around 213.4 nm and 221.6 nm, respectively. At relatively long wavelength absorption occurs at high concentration while the saturation occurs at the shorter wavelength. This leads to the most accurate detection of NH_3 below 450 ppm at 213.4 nm and for 400-1000 ppm at 221.6 nm. Because the UV absorption of N_2O is too weak, as shown in Fig.8 for the spectra of 67 ppm, NO_2 can not be detected with reasonable accuracy using UV absorption. In the absence of NH_3 injection, a electrochemical analyser is used to detect NO_x. In the presence of NH_3, only NO is detected using UV absorption.

3.2 Calibrations

In principle, gas concentration can be calculated using the absorption cross sections. Unfortunately, data of UV absorption cross sections for NO, SO_2 and NH_3 are limited. The most reported in the literature are the total absorption values which are generally higher than the differential ones. In view of this obstacle, the calibration is directly assessed by comparing the results with an electrochemical analyser for NO and SO_2, and calibrated gas flow controllers for NH_3. Since a part of NO spontaneously converts into NO_2 in air, NO calibration is made only with flue gas. For SO_2 and NH_3, the calibrations are made with air to avoid reactions with water. It can be seen, in fig.9, the absorption ($\sigma C(m^{-1})$) of NO at 226.2 nm and NH_3 at 213.4 nm strongly depends on the concentrations while NH_3 at 221.6 nm and SO_2 at 300 nm present almost linear absorption-concentration relationships. For signal NO, SO_2 and NH_3 gas with 0-450 ppm(a) and 0-1200 ppm(b) injected in flue gas or air flow, the calibration curves are given in fig.9. The measurements of NO and SO_2 have an error of less than 3% (or 10 ppm for 300 ppm whichever is the highest). For ammonia it is slightly higher with 5% at 900 ppm, but concentrations downto 1 ppm can be observed at 204nm.

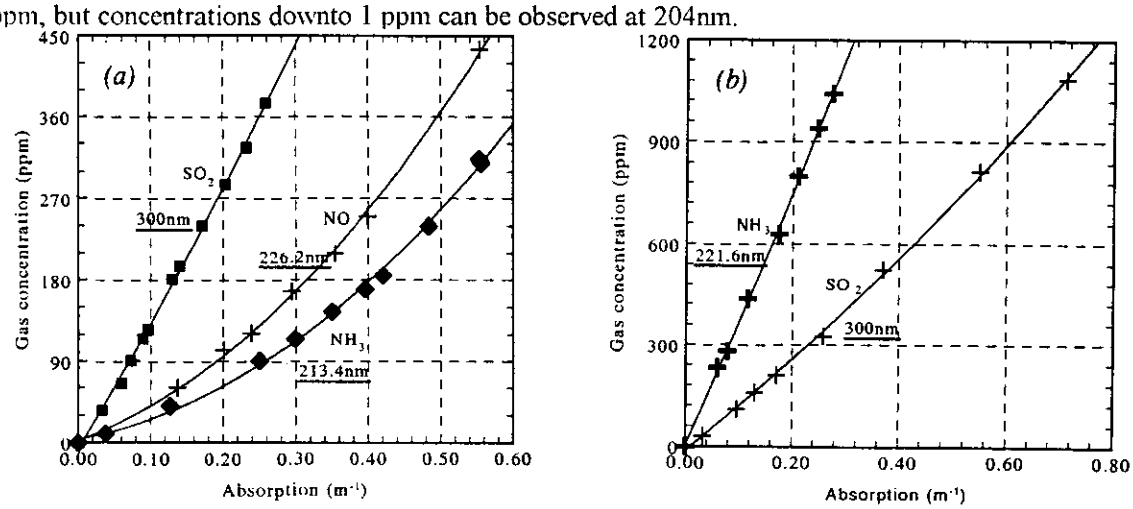

Fig 9: Calibrations of NO, SO_2 and NH_3 at lower (a) and higher (b) concentrations.

A problem in gas mixture is the overlap of SO_2 absorption with NH_3 and NO in the region 200-237.5 nm (Fig.10). To overcome this problem, the SO_2 fractional absorption is subtracted from the overlap at the wavelengths for NO and NH_3 detection, respectively, since SO_2 is firstly detected at around 300 nm without this difficulty. Additional errors caused by this cross calibration are negligible. Fig.11 gives SO_2 concentration-absorption calibrations at 213.4 nm and 221.6 nm. It can be seen that when SO_2 concentration is less than 25 ppm, there is actually no overlap at 226.2. Besides the influence factors mentioned above, other possible factors are also examined. The total gas flow and the stability of Xe-lamp signal used in the cleaning measurements have no apparent influence on the measurement. But, during the following experiments, the temperature in absorption cell, the settings of monochrometer and PM should be fixed at the values used in the calibrations. The absorption measurement must be corrected to account for the difference between calibration and experiment temperatures of the gas flow in the reactor using the ideal gas low.

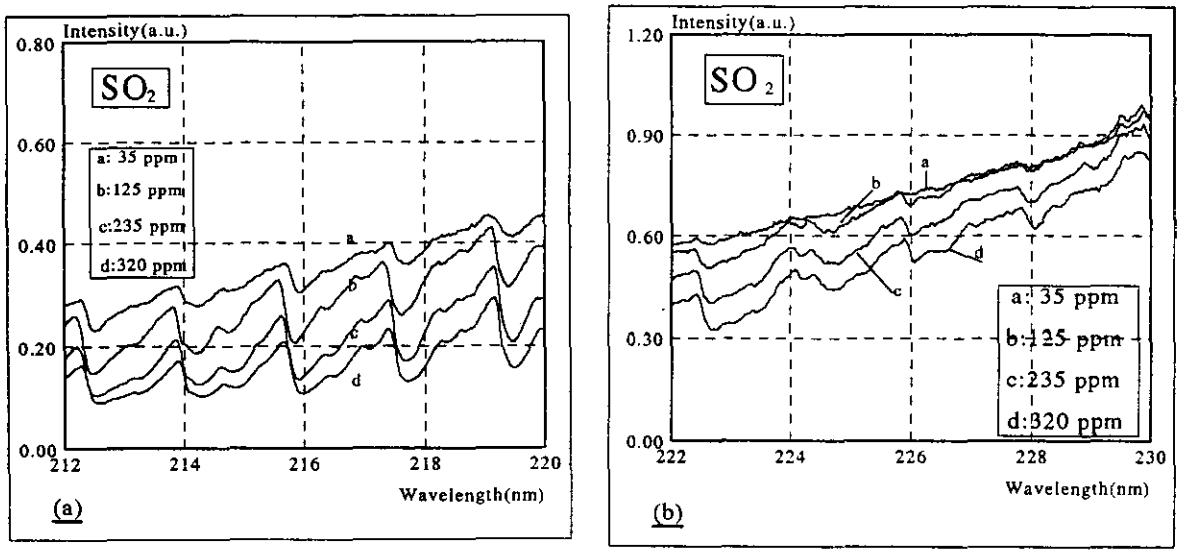

Figure 10: SO_2 absorption spectrum in the region of 212-220 nm (a) and 222-230 nm (b) for four concentrations.

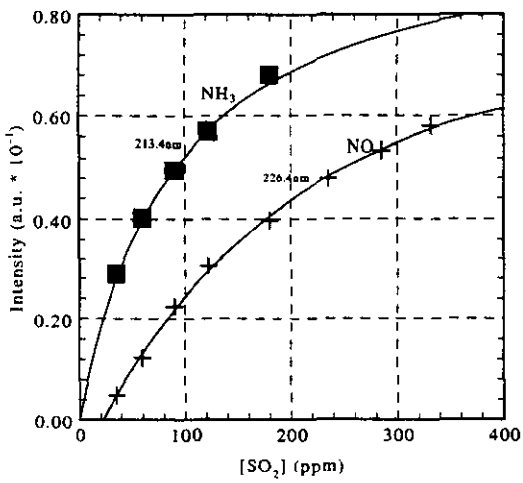

Figure 11: Cross calibrations of SO_2 absorption at 226.2 nm for NO detection and 213.4 nm for NH_3 detection.

4. Cleaning measurements

4.1 Removal of NO/NO_x

4.1.1 DC bias effect

For optimizing the energization, the effect of dc bias on the removal of NO and NO_x (the sum of $NO+NO_2$) energy efficiency is firstly investigated in flue gas at 130 °C and 25 Nm^3/h (9.6 s residence time) with 3 % O_2, 10 % CO_2 and about 20 % H_2O. The initial NO/NO_x concentrations are 350 and 380 ppm, resp.. Test results are graphically presented in Fig.12. It can be clearly seen that both NO and NO_x removal performance is better with 20 kV bias than that with 30 kV bias at the same energy input. For instance, at 6 Wh/Nm^3 energy input, about 38% NO and 23% NO_x (energy cost:40 eV/NO, 61eV/NO_x) are removed in the case of 20 kV dc bias but only 30% NO and 18% NO_x (energy cost: 50 eV/NO, 76 eV/NO_x) in the case of 30 kV dc bias.

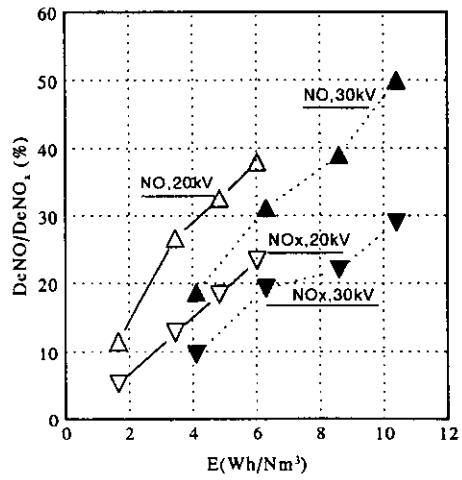

Figure 12: Comparison of NO/NO_x removal at 20 kV and 30 kV bias. ($T=130$ °C , t_{res} =10 s, flow=25 Nm^3/h, $[NO]_i$= 350 ppm, $[NO]_x$= 380 ppm, O_2= 3 %, CO_2 = 10 %)

In 80 °C flue gas (12% O_2; 2.5 % CO_2) with 15 s residence time, the performance of NO/NO_x removal at 30 kV bias is compared with 15 kV dc bias in Fig.13. The initial NO/NO_x concentrations are 330 and 360 ppm, respectively. At about 5.3 Wh/Nm^3, the removal rate with 15 kV bias is almost two times higher than that with 30 kV. Correspondingly, the energy cost is reduced a factor two at the same removal rate.

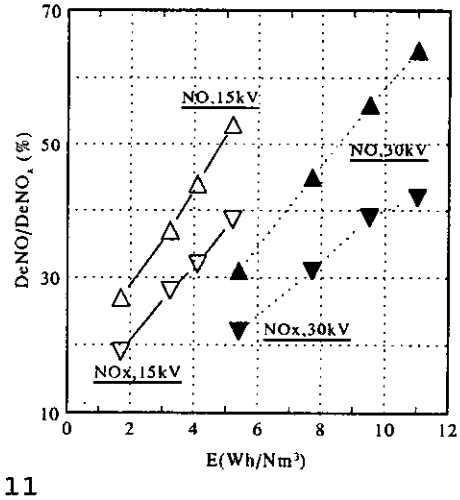

Figure 13: Comparison of NO/NO_x removal at 15 kV and 30 kV bias. ($T=80$ °C, t_{res}=15s, flow=15 Nm^3/h, $[NO]_i$ = 330ppm, $[NO_x]_i$=365ppm, O_2=12 %, CO_2=2.5 %)

In 70 °C standard flue gas with 30 s residence time, the removal performances of NO/NO_x with and without dc bias are compared in fig.14. The better results have been obtained in the absence of a bias.

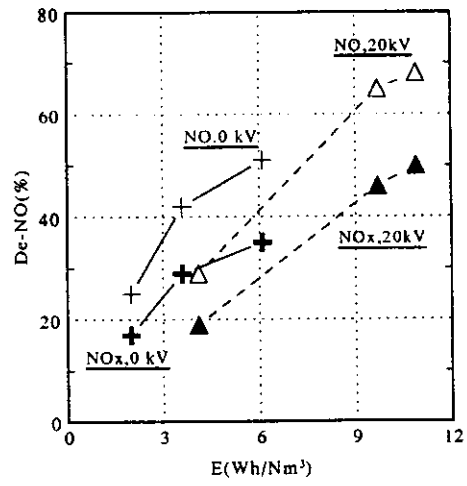

Figure 14: Comparison of NO/NO_x removal at 0 kV and 20 kV bias in standard flue gas. (T= 70 °C, t_{res}=30s, flow=9 Nm^3/h, $[NO]_i$= 300 ppm, $[NOx]_i$=325 ppm.)

In 80 °C flue gas with standard composition at a gas residence time of 30 s, the relationships of energy cost vs. dc voltage in the case of the removal of 32 % NO and 15 % NO_x are measured. The initial concentrations of NO and NO_x are 330 ppm and 360 ppm, respectively. As shown in fig.15(a), the energy cost for removal of both NO and NO_x increase slightly with the increase of dc voltage upto 20 kV (The dc corona inception voltage of this electrode system is around 18 kV). Beyond 20 kV, this increase becomes stronger. The energy consumption per removed NO or NOx at 30 kV is almost a factor two higher than that at 20 kV. In the case of 50 % NO removal, a difference is increased a factor three at a gas residence time of 15 s. This result is contrary to data obtained by Belousova[9]. Figure 15(b) shows the effects of dc bias on the injection energy and chargers of the corona discharge per pulse and discharge power. It is evident that the general trend of all curves in both figures presented are almost the same. This indicates that the use of dc bias mainly increases the discharge energy input, but certainly above the inception voltage this additional energy is not used efficiently and therefore leads higher energy cost for NO/NO_x removal. This finding is of practical importance for optimizing the energization.

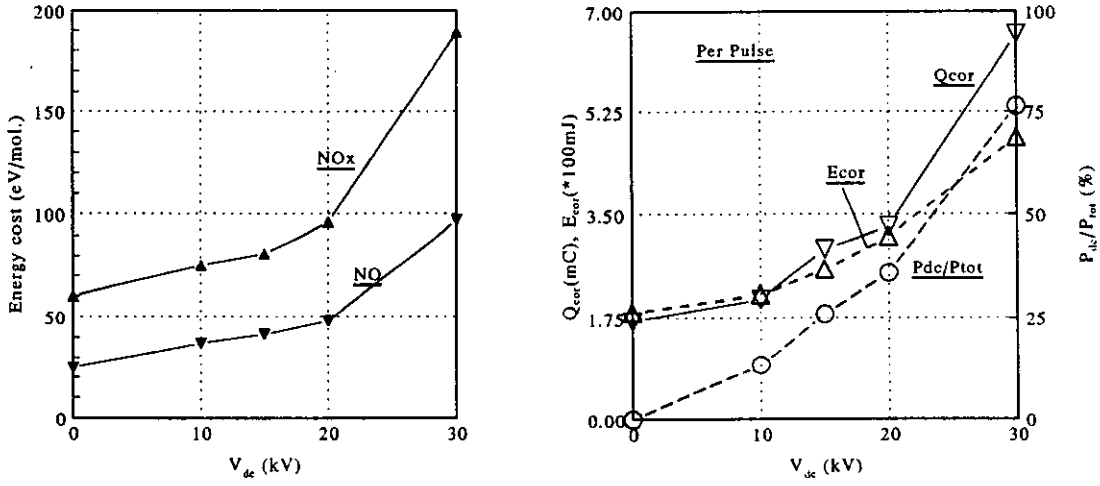

Figure 15: Effect of dc bias on the removal of about 32 % NO and 15 % NO_x in standard flue gas (T=80 °C, t_{res} =30 s, flow= 9 Nm^3/h, $[NO]_i$= 330 ppm, $[NO_x]_i$=360 ppm).

4.1.2 **Residence time effect**

In 70 °C standard flue gas with 300 ppm NO injection (320 ppm NO_x), the NO/NO_x removal is respectively tested at the residence time of 6 s and 30 s with 20 kV dc bias. The results are plotted in fig.16. Due to the power limitation of the supply, the removal rate at 6 s can not be compared with that that at 30 s at the same energy input. But, with a curve-fitting, all data points are located on one smooth curve. This implies that the removal performances have no apparent difference between both cases. At 80 °C standard flue gas with 320-330 ppm NO injection, the results of NO removal at the residence time of 30 s and 15 s are compared in fig.17 with 15 kV and 20 kV dc bias, respectively. An apparent difference is found for removal rates with both residence times at same dc bias. The removal performance at 15 s is better than that at 30 s.

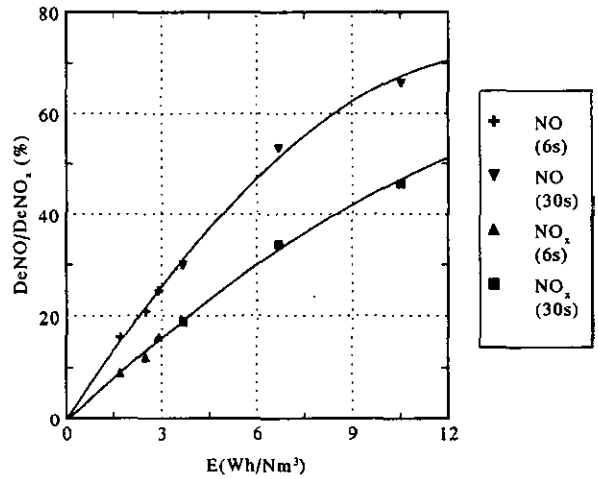

Figure 16: NO/NO_x removal in standard flue gas with the residence time of 6 s and 30 s.
(T=70 °C , $[NO]_i$= 300 ppm, $[NO_x]_i$=320 ppm, V_{dc}=20 kV)

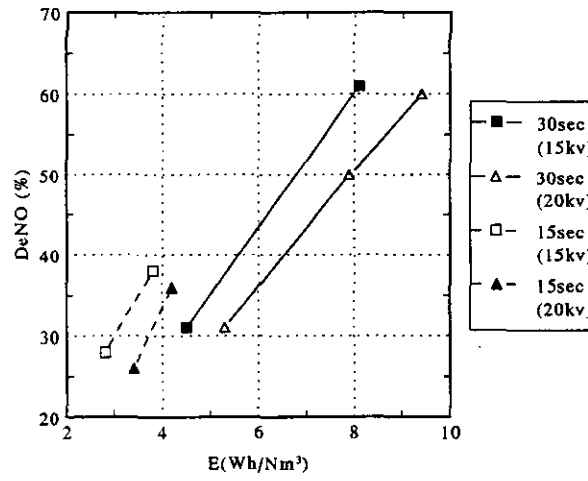

Figure 17: Comparison of NO removal in the standard flue gas with the residence time of 15 s and 30 s.
(T=80 °C, $[NO]_i$=330 ppm)

In order to clarify the effect of residence time on the removal performance, the further measurements are conducted for 30% removal of 320-330 ppm NO with dc voltage of 15 kV and 20 kV, respectively. In this case, the standard flue gas with 80 °C is used. The input of discharge energy is varied with the change of the pulse frequency. As shown in fig.18, the required energy for 30% NO removal first goes down with increasing residence time. When reaching a minimum at around 15 s, the energy goes up. In the period of 30-60 s, this specific energy is almost the same as that at 6 s. At 15 s residence time, the energy cost for the NO removal can be at least reduced by 30 % in both cases of 15 kV and 30 kV dc bias. But, the required energy at 15 kV is 25% less than that at 30 kV. In the region of the longer residence time, the higher energy requirement could be explained by the formation of NO due to reverse reaction of NO_2 and radical O which offsets the NO reduction. For the shorter residence time, the conversion of 30 % NO requires active radicals and therefore needs more energy input, which has been confirmed by using chemical kinetics calculations [10]. This result suggests that there is a optimum residence time for the removal of NO/NO_x in a certain volume of the discharge reactor.

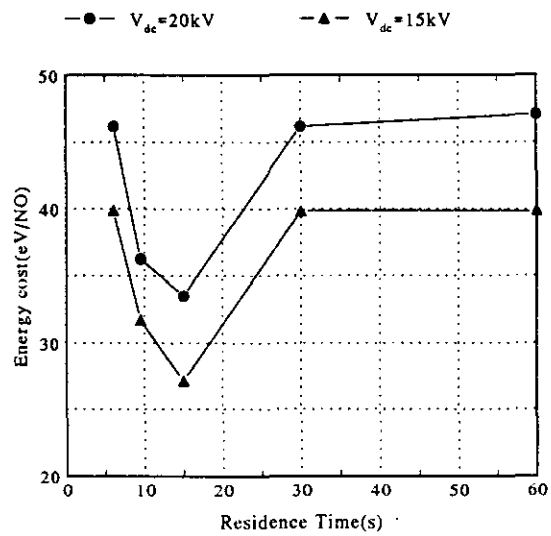

Figure 18: Effect of gas residence time on the removal of about 30 % NO in the standard flue gas. (T=80° C, $[NO]_i$=330ppm).

The optimal residence time is around 15 s.

4.1.3 O_2 and H_2O effect

The flue gas used in most cases has 6 % O_2 and 16 % H_2O. It has known that the O_2 and H_2O contents have a pronounced influence on the removal of NO/NO_x. In the present experiments, this effect is also examined in 80 °C flue gas with 15 s residence time. The initial concentration of NO/NO_x are 330 and 360 ppm, respectively. The removal performance in the flue gas with 6 % O_2 and 16 % H_2O are compared with that in the flue gas with 12 % O_2 and 10% H_2O in Fig.19. The effect of CO_2 content on the removal of NO/NO_x is small. As seen in fig.19, when the total content of O_2 and H_2O is the same, the removal rate at 12 % O_2 content is better than that at 6 % O_2. In the region of energy input in fig.19 with 15 kV ac bias, the removal rate of NO/NO_x are improved about 30 %. This is in general in agreement with the earlier small-scale measurements by Tas [11]. Since a real flue gas has a O_2 content of around 6 %, the removal of NO/NO_x can not been further optimized with gas composition.

Figure 19: Effect of O_2 and H_2O on the removal of NO/NO_x in the case of same total content (22%) of O_2 and H_2O. (T=80 °C, t_{res} =15 s, flow=19 Nm^3/h, $[NO]_i$=330ppm, $[NO_x]_i$= 360ppm, V_{dc}=15kV).

The removal rate at 12 % O_2 content is better than that at 6 % O_2.

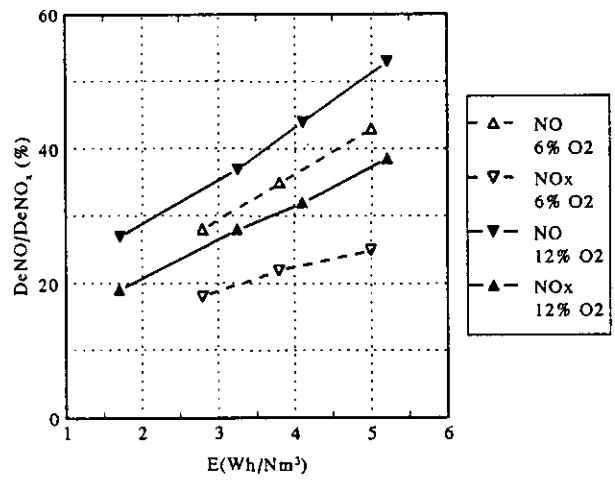

4.1.4 Temperature effect

NO/NO_x removal experiments are performed with a dc bias of 30 kV, respectively. At 130 °C, the flue gas conditions are: 3 % O_2, 20 % H_2O, 9.6 s residence time, 350 ppm NO and 380 ppm NO_x . At 80 °C, these are :10 % O_2, 12 % H_2O, 16 s residence time,320 ppm NO and 360 ppm NO_x . Although the gas conditions are not the same in 130 °C and 80 °C flue gases, the apparent influence on the NO/NO_x removal performance in fig. 20 are believed to be mainly ascribed to the gas temperature. At 80 °C , more than 90% NO is removed when 11 Wh/Nm^3 discharge energy is input, resulting in a energy cost of less than 35 eV/NO. In comparison with the results at 130 °C, this is almost a factor two better. The temperature dependence presented here is consistent with the previous work at EUT [4]. In combination with earlier work, it suggests that the optimum gas temperature for NO/NO_x removal is just above the condensation point of water.

Figure 20: Temperature effect on the removal of NO/NO_x. (flue gas 1: T=80° C, t_{res} = 16s, $[NO]_i$ = 320ppm, $[NO_x]_i$= 350ppm, O_2=10 %, H_2O=12 % ; flue gas 2: T=130° C, t_{res}=10s, $[NO]_i$ = 350 ppm, $[NO_x]_i$=380 ppm, O_2=3%, H_2O=20%).

The lower temperature is better for removal of NO and NO_x.

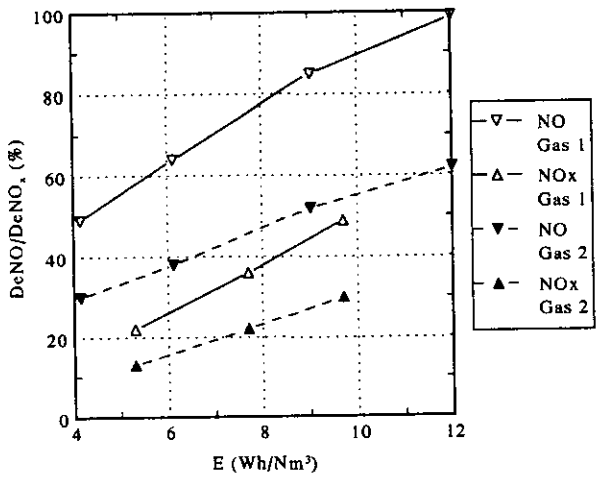

4.2 Removal of SO_2

The SO_2 removal tests are conducted in room air and flue gas, and in the cases with and without NH_3 injection, respectively.

4.2.1 Removal of SO_2 in air

In air of 24 °C and 23 % RH, 300 ppm SO_2 was introduced into a 22.4 Nm^3/h air flow. As shown in Fig. 21, SO_2 removal rate is only 10-30 % by the corona discharge alone. At 7.2 Wh/Nm^3 energy input, 480 ppm NH_3 injection produces 55 % SO_2 removal rate and no slip NH_3 was observed. At 8 Wh/Nm^3, 600 ppm NH_3 injection produces 88 % SO_2 removal rate and no slip NH_3 was observed. In the case of 600 ppm NH_3, SO_2 removal rate goes through a maximum of 90 % at 1.6 Wh/Nm^3 and then starts to slightly go down with increasing power density. But slip NH_3 is always decreasing with increasing power density. The removal results of SO_2 obtained here are in agreement with the those obtained by Chang J. S. [12].

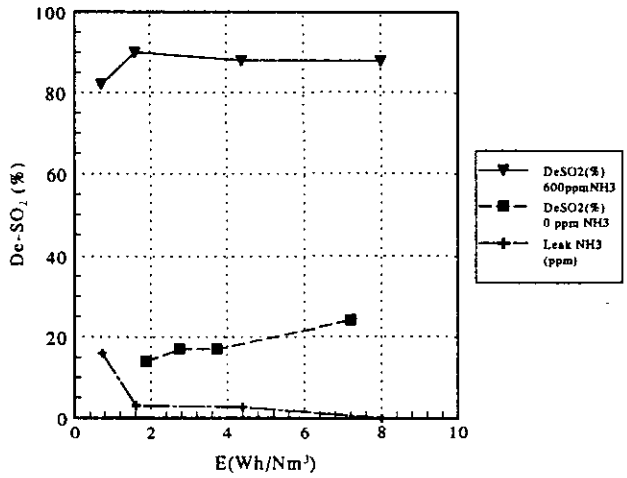

Figure 21: The removal of SO_2 in air flow with and without addition of NH_3. ($T=24°C$, $t_{res}=14s$, flow =22 Wh/Nm^3, $RH=23\%$, $[SO_2]_i=300ppm$).

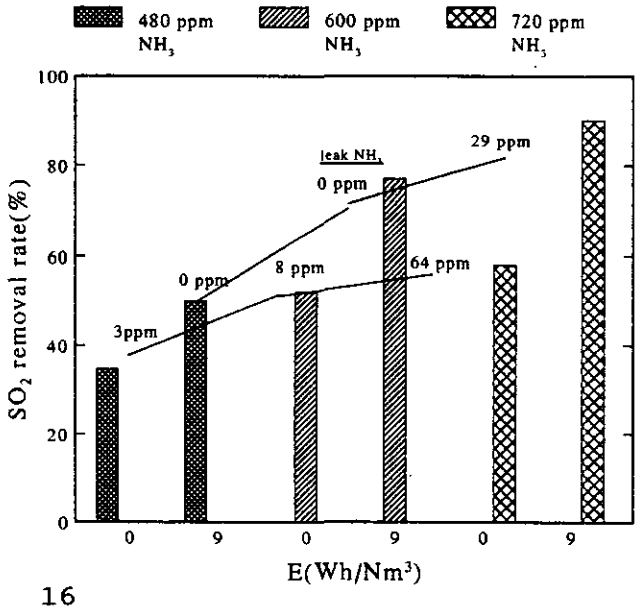

Figure 22: Comparison of the removal of SO_2 in presence of NH_3 in air without and with discharge. ($T=70$ °C, $t_{res}=14s$, flow=19 Nm^3/h, $[H_2O]=16\%$, $[SO_2]_i=300ppm$).

The auto-thermal reaction is dominant for SO_2 removal.

In 70 °C air with 300 ppm SO_2, the removal rates are compared in the cases with and without discharge energy input for the injection NH_3 concentration of 480 ppm, 600 ppm and 720 ppm. This measurements show several trends. The first is that more NH_3 injection leads to higher SO_2 removal rate, both with and without discharge. A clear trend in the leak NH_3 is that the discharge reduces the leak of NH_3. Thirdly, thermal reaction without discharge can remove 36-58% of 300 ppm SO_2 in air, also depending on the amount of NH_3 injection.

4.2.2 Removal of SO_2 in flue gas

The removal of SO_2 is also tested in a wide region of gas condition (H_2O: 1-16 %, Temp.: 24-130 °C, NH_3: 480-720 ppm). Without NH_3 injection SO_2 removal rate is never more than 30 % at energy input upto 10 Wh/Nm^3 in both air and flue gas. But, in the case of NH_3 injection, SO_2 removal significantly increases with the increase in the amount of NH_3 (fig.24). The gas temperature and water content have an obvious influence for SO_2 removal with NH_3 injection. At 76 °C and 16 % H_2O, more than 99% SO_2 removal rate is achieved at 3 Wh/Nm^3 with 720 ppm NH_3 injection. In flue gas, it is also observed that the corona discharge hardly improves the SO_2 removal, but strongly reduces NH_3 slip. Slip of NH_3 also increases with increasing NH_3 concentration. SO_2 removal by thermal reaction of SO_2-NH_3 without discharge is much more effective than that by energized corona process in air and flue gas, but slip NH_3 is much higher in the thermal reaction. These experiments indicate that the high discharge energy is required for complete NH_3 removal. This is quite similar to the results of Civitano [3].

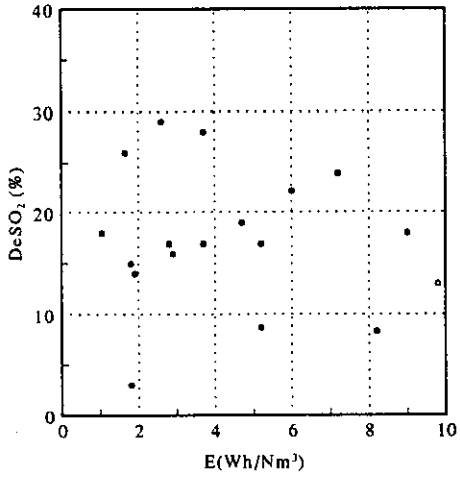

Figure 23: The removal of 300ppm SO_2 in a wide condition region (H_2O:1%-16%, T:24-130 °C) without NH_3 injection.

SO_2 removal rate is never more than 30% at energy input upto 10 Wh/Nm^3.

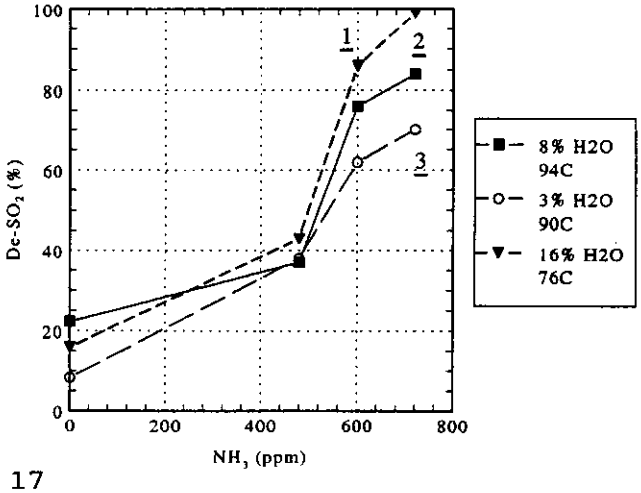

Figure 24: Effect of NH_3 injection on the removal of 300 ppm SO_2 in flue gas (1: T=76° C, t_{res} =6 s, H_2O = 16 %, E= 3 Wh/Nm^3; 2: T=94 °C , t_{res} =12 s, H_2O=8 %, E= 6 Wh/Nm^3; 3: T=94° C , t_{res} =12 s, H_2O=3%, E=7 Wh/Nm^3).

4.2.3 History effect

During the SO_2 removal experiments with NH_3 injection, it is observed that the SO_2 removal has a strong history effect. Two typical sets of tests are shown in fig.25. In the case of 720 ppm NH_3 injection into gas flow with a gas temperature of 90 °C and a gas residence time of 12 s, the test is started at 7 Wh/m^3 after 10 mins. This time is a little longer than the time required by the gas to flow through the whole system and reach the absorption cell. It is observed that the SO_2 removal rate increases from 70% at 7Wh/Nm^3 with a decrease of the energy input. At 1.9 Wh/Nm^3, a 84% SO_2 removal rate is obtained. Then the corona is off, the removal rate goes down to 74%. The leak NH_3 always decreases with increasing energy input. In the second set of tests, a flue gas of 70 °C and a gas residence time of 30 s is used. The tests are started 1.5 h after 600 ppm NH_3 is injected. The time interval between two data points is 20 mins for each increase of energy input. In this procedure, the SO_2 removal rate always increases with the more energy input. At 7.7 Wh/Nm^3, a 97% removal of 300 ppm SO_2 is detected. The NH_3 slip also decreases from 17 ppm to less than 1 ppm. History effects like this are also reported by Li [13].

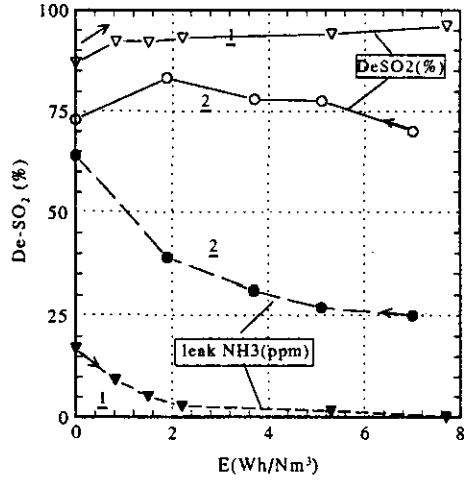

Figure 25: History effect for the removal of SO_2 in flue gas.
(1: T=70 °C, t_{res} = 30 s, H_2O=18%, [NH_3]= 600 ppm;
2: T=94 °C , t_{res} =12 s, H_2O=3%, [NH_3]=720 ppm)

The arrow indicates the time sequence of the data points. History effect is beneficial for SO_2 removal.

4.3 Combined removal of NO and SO_2

4.3.1 SO_2 effect on DeNO/DeNO_X

The effect of SO_2 injection on the NO/NO_x removal is tested in a 70 °C flue gas with a residence time of 30 s. The results obtained at an energy input of 7 Wh/Nm^3 is plotted in fig.26. In this case, a 20 kV dc bias and 350 ppm NO_x (320 ppm NO) are used. NO removal rate is 52% without SO_2 injection, resulting in 40 eV/NO. In this case, the reduction of NO_x is 37 % (50 eV/NO_x). When SO_2 is introduced into the gas flow, NO and NO_x removal rates are enhanced. At 900 ppm SO_2, NO and NO_x removal rates increase to 78 % and 71 %, respectively, corresponding to energy cost of 24 eV per removed molecule for both NO and NO_X. By comparing figure 27(a) with figure 13-14, it is noted that in the presence of SO_2 the improvements of the removal NO_x is much stronger. This implies that SO_2 can reduce the reverse reaction in the removal of NO_x.

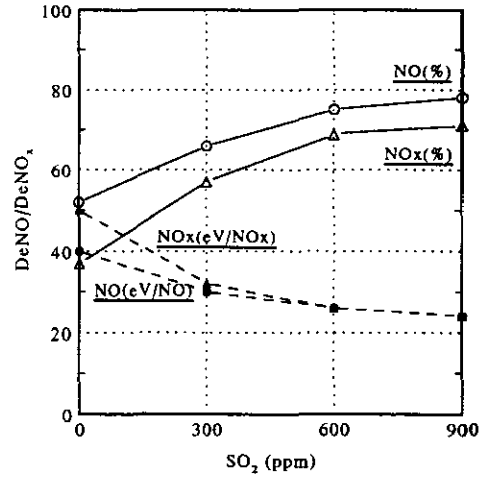

Figure 26: Effect of SO_2 injection on the removal of NO and NO_x in the standard flue gas (T=70 °C, t_{res} =30 s, flow= 9 Nm³/h, E= 7 Wh/Nm³, V_{dc}=15 kV, $[NO]_i$=320 ppm, $[No_x]_i$=350 ppm).

The presence of SO_2 has a positive effect on NO/NO_x removal.

4.3.2 Synergetic effect of SO_2, NO and NH_3

It is also found that NO concentration decreases from 308 to 260 ppm with 600 ppm SO_2 injection without corona discharge. However, NO concentration goes back in this case to its initial value when 1200 ppm NH_3 is also injected. With corona discharge, the NH_3 and SO_2 injection

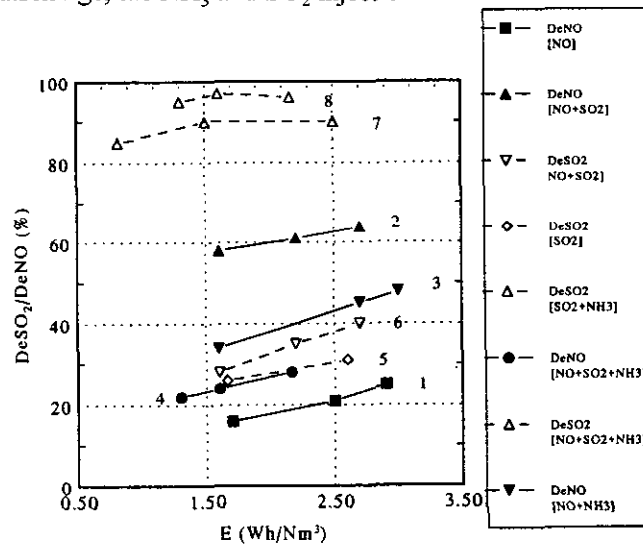

Figure 27(a): Synergetic effect for the removal of SO_2 and NO in standard flue gas. (T= 70 °C, t_{res} =6 s, V_{dc}=20 kV, $[NO]_i$=300ppm, $[SO_2]$=300ppm, $[NH_3]_i$=600 ppm).

<u>DeNO</u>: (1)-[NO], (2)-[NO+SO_2], (3)-[NO+NH_3], (4)-[NO+SO_2+NH_3];

<u>DeSO$_2$</u>: (5)-[SO_2], (6)-[SO_2+NO], (7)-[SO_2+NH_3], (8)-[SO_2+NO+NH_3].

enhance the NO conversion, respectively but also together. The typical results in 70 °C flue gas with 6 s residence time is graphically presented in Fig. 27. It can be seen that 300 ppm SO_2 injection improves NO removal with a factor three. 600 ppm NH_3 injection improves NO removal with a factor two, but leak NH_3 is quit high (190ppm at 3 Wh/Nm³; 280 ppm at 2.7 Wh/Nm³). The positive effect of NH_3 on NO removal is in good agreement with recent results of Chang [12] and Niessen [14]. When SO_2 and NH_3 are simultaneously introduced into gas flow, the enhancement of NO removal rate is about 1.5, which is lower than in the case of respective injection of SO_2 and NH_3. Without NH_3 injection, SO_2 removal rate is 22-25 % at energy input of 1.5-2.5 Wh/Nm³. NO presence has a small positive effect on SO_2 removal. In the presence of NH_3, but without NO injection, 90 % SO_2 removal rate is obtained at 1.5 Wh/Nm³ with 5 ppm NH_3 slip. When three species exist together, SO_2 removal rate is more than 99 % with leak NH_3 of 5-13 ppm. Leak NH_3 is less with more energy input.

4.3.3 NH_3 effect on the removal of SO_2 and NO

In 70 °C standard flue gas with 6 s residence time, the effect of NH_3 injection on the removal of NO (300 ppm) and SO_2 (300 ppm) is investigated. As shown in fig. 27(b), the SO_2 and NO removal rates increase with increasing NH_3 injection. When NH_3 concentration increases from 600 to 900 ppm at about 2 Wh/Nm^3, the NO removal rate increases from 25 % to 50 %, correspondingly leads to a decrease of energy cost from 26 eV/NO to 12 eV/NO. But, in this case, the leak NH_3 also increases with increasing NH_3 injection (5ppm at 600 ppm injection; 140 ppm at 900 ppm injection).

Figure 27(b): Effect of NH_3 injection on the simultaneous removal of SO_2 and NO in standard flue gas

(T=70 °C, t_{res} =6 s, $[NO]_i$=300ppm, $[SO_2]_i$=300 ppm, V_{dc}= 20 kV)

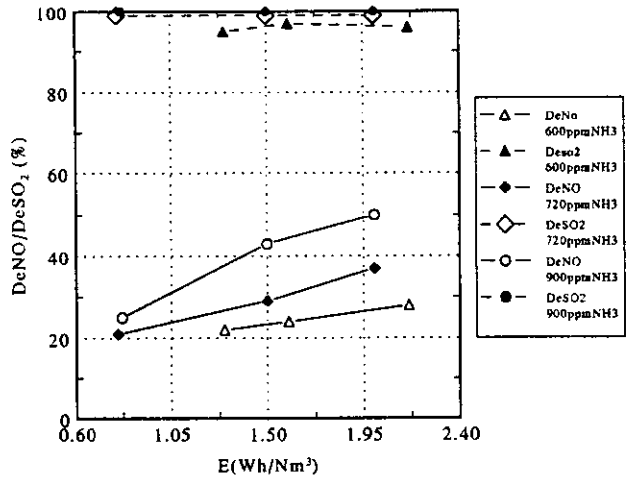

4.3.4 Enhancement of synergetic effect

In order to effectively use the positive effect on NO removal, NH_3 is injected at the location of 70 cm from the exit of the corona reactor (location 2 in fig.1). The results at 80 °C flue gas with 30 s residence time is plotted in fig. 28. SO_2 from 300 to 1000 ppm is injected with corresponding stoichiometric NH_3 of 600-2000 ppm. NO concentration is 320 ppm. Energy input is 7 Wh/Nm^3 with 15 kV dc. It is seen that NO removal rate increases with SO_2 and NH_3 concentration. When

Figure 28: Removal of SO_2 and NO from standard flue gas in the case <u>of NH_3 injection later</u> (T =80 °C, t_{res}= 30s, $[NO]_i$=320ppm, $[NH_3]_i$=2$[SO_2]_i$, E=7 wh/Nm^3, V_{dc}=15kV).

NO removal of 81% (23 eV/NO) and SO_2 removal of over 98% with less than 5 ppm leak NH_3 have been obtained.

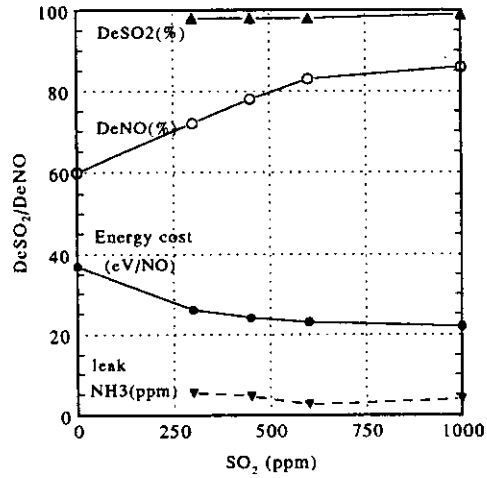

SO_2 concentration reaches 600 ppm, NO removal rate increases from 61 % (without SO_2 and NH_3 injection) to 81 %. Correspondingly energy cost reduces from 37 to 23 eV/NO. The further increase of SO_2 and NH_3 does not give a further increase of NO removal. In this set of measurements, SO_2 removal rate is always over 98% and leak NH_3 is always less than 5 ppm.

When 300 ppm SO_2 is injected at the location of 70 cm (location 2 in fig.1) form the rector exit and NO (320 ppm) and NH_3 (changed from 600-1200 ppm) are injected before the reactor (location 1 in fig.1), the NO removal is also improved at 7.5 Wh/Nm^3 as shown in fig. 29. The removal rate of 97 % for SO_2 and 81 % for NO (25 eV/NO) are obtained at 900 ppm NH_3 injection. The leak NH_3 is only about 2 ppm.

*Figure 29: Removal of SO_2 and NO from standard flue gas in the case of **SO_2 injection later**. (T=80 °C, t_{res}=30s, $[NO]_i$=320 ppm, $[SO_2]_i$= 300 ppm, E = 7.5 Wh/Nm^3, V_{dc}=15kV).*

The removal rate of 97 % for SO_2 and 81% for NO (25 eV/NO) with 2 ppm leak NH_3 are obtained at 900 ppm NH_3 injection.

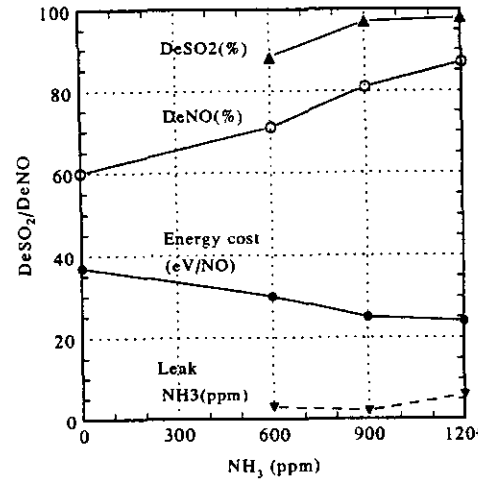

In the case of 15 s gas residence time and 3.7 Wh/Nm^3 energy input with 15 kV dc bias, the effect of NH_3 injection before the reactor is plotted in fig. 30. Without SO_2 injection, 300 ppm NH_3 injection improves NO removal with a factor two and a half, i.e., removal rate increases from 31 % without NH_3 injection to 73 % with NH_3 injection, resulting in a decrease of energy cost from 32 to 14 eV/NO.

*Figure 30: Effects of NH_3 and/or **SO_2 injection** (later) on the removal of NO from the standard flue gas. (T=80 °C, t_{res} = 15 s, flow = 19 Nm^3/h, E= 3.7 Wh/Nm^3, V_{dc}=15 kV).*

NH_3 injection improves NO removal rate from 31 % to 73 % (14 eV/NO) with 1.3 ppm leak NH_3. SO_2 and NH_3 together improves NO removal rate to around 68 % (15 eV/NO).

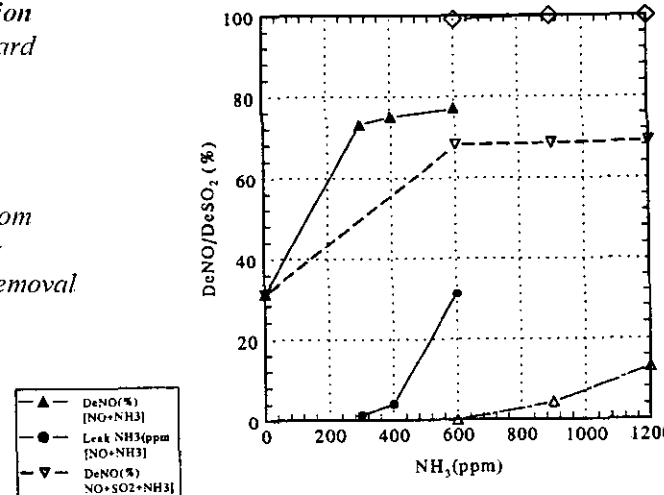

Leak NH_3 increases from 1.3 to 31 ppm with increasing NH_3 concentration from 300 to 600 ppm. When 600-1200 ppm NH_3 and 300 ppm SO_2 are injected simultaneously but at different locations, this improvement for NO removal becomes a little smaller. The NO removal rate is around 68 % in this case, corresponding to a energy cost of 15 eV/NO. SO_2 removal rate is always more than 99 % and leak NH_3 increases from less than 1 ppm to 13 ppm with increasing the injection of NH_3. As compared with the results in fig.27, the positive effect of SO_2 and NH_3 together on NO removal is greatly enhanced with the adjusting the locations of gas injections. In this case, it is interesting to find that the NO and SO_2 concentrations at the exit of the system change with the measurement time. At 3.7 Wh/Nm^3 energy input, the NO concentration firstly goes down to a minimum of 30 ppm (92 % removal) at 20 mins and then goes up to a maximum of 120 ppm (63 % removal). After 50 mins, the NO concentration reaches a stable level of around 105 ppm (68 % removal, 15 eV/NO). SO_2 and NH_3 concentrations always decrease with the time. After 50 mins, almost 100 % SO_2 is removed without NH_3 slip. At 4 Wh/Nm^3 energy input, a same change in trend for NO and SO_2 concentrations is observed. The stable level is at 50 ppm NO (85 % removal, resulting in 12.6 eV/NO). The 95 % of 300 ppm SO_2 is finally removed with less than 3 ppm NH_3 slip. This is up to now our best result. Such a time-dependence of the removal of SO_2 and NO with NH_3 injection is probably related to the formation of particles and heterogeneous reactions. The results presented from fig.28 to fig.31 indicates that the NH_3 and SO_2 injections at the different location on the reactor is beneficial for the improvement of energy efficiency of NO removal.

Figure 31: The variation of NO and SO_2 concentration with the measurement time. (T=80 °C, t_{res} =15 s, standard flue gas, SO_2 injection later, $[NO]_i$=330 ppm, $[SO_2]_i$=300ppm, $[NH_3]_i$=600 ppm, V_{dc}=15 kV).

85% NO (12.6 eV/NO) and 95% SO_2 is finally removed with less than 3 ppm NH_3 slip at 4 Wh/Nm^3.

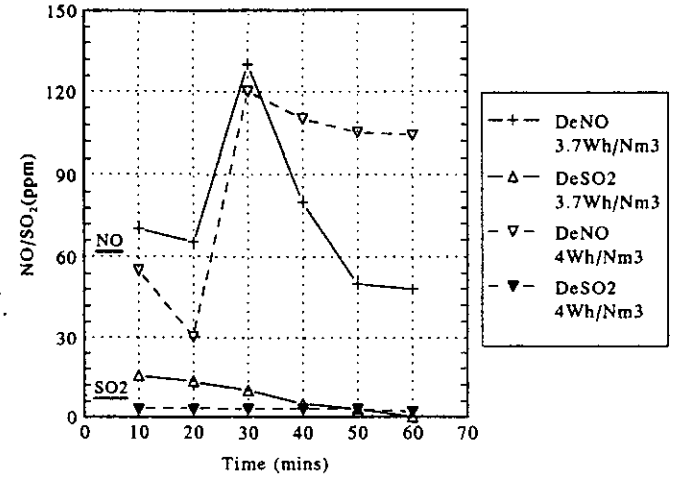

5.Two-stage cleaning measurements

5.1 NO and NO_x removal

With two corona reactors in series, the experiment on DeNO/DeNO_x is conducted in 70 °C standard flue gas with 300 ppm NO (320ppm NO_x) and 30 s residence time (18 Nm^3/h flow). The results are plotted in fig. 32 in comparison with the results obtained in single-stage at the same residence time (30 s, 9 Nm^3/h flow) and same gas conditions. As seen in fig.32, the removal rates of NO and NO_x in two-stage are a factor two lower than that in single-stage at the same discharge power input. But, the energy costs of NO and NO_x removal in both cases are almost the same since the specific energy (in unit Wh/Nm^3) also decreases a factor two in the two-stage. When the residence time in the two-stage system is increased to 60 s, no apparent difference is found for NO and NO_x removal.

Figure 32: Comparison of the removal of NO and NO_x with single-stage and double-stage in the standard flue gas (T=70 °C, t_{res}= 30 s, $[NO]_i$=300 ppm, $[No_x]_i$=320 ppm, V_{dc}= 20 kV).

The removal rates of NO/NO_x in two-stage system are a factor two lower than that in single-stage system at the same discharge power.

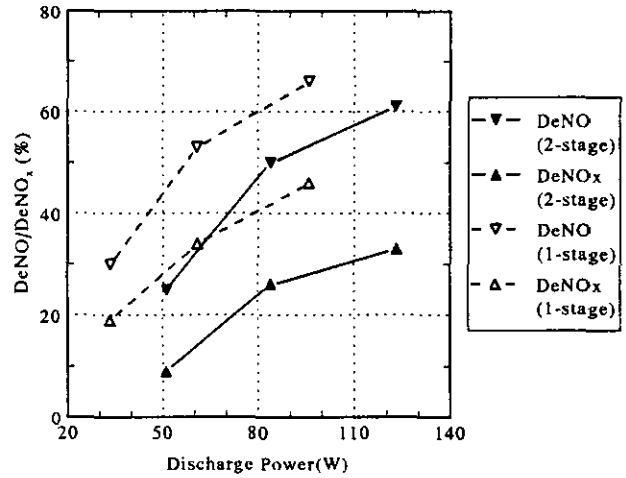

5.2 Combined removal of SO_2 and NO_X

The double-stage measurements of simultaneous removal of SO_2 (300 ppm) and NO (310 ppm) in the presence of NH_3 (600 ppm) are carried out in a 70 °C flue gas with a residence time of 30 s. The flow velocity is about 10 m/min, resulting in an interruption time of 5 s in-between two chambers. As compared with one-stage measurements with the same gas residence time, the NO removal rate in the two-stage is a factor two lower than that in the single-stage. As given in Fig.33, at about

Figure 33: Comparison of NO removal with single-stage and double-stage in the standard flue gas in presence of NH_3 and SO_2 (T=70 °C, t_{res} =30s, $[NO]_i$=300ppm, $[SO_2]_i$=300 ppm, $[NH_3]_i$=600ppm, V_{dc}=20kV).

The NO removal rate in the two-stage is a factor of two lower than in the single-stage.

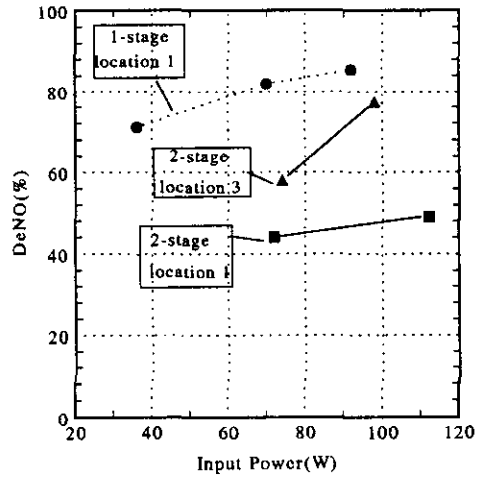

70W power input, the NO removal rate are 82 % and 45 % for single and double stage treatments, respectively, resulting in about 25 eV/NO for both. This is similar to that without SO_2 and NH_3 injection. When NH_3 is injected in-between stages (location 3), the performance of NO removal rate is improved as well as energy efficiency. At 70 W power input, NO removal rate is 58 %, corresponding to an energy cost of 22 eV/NO. But, in general, the NO removal rate is still lower than that in single-stage with the same energy input. This is quite different from the result using electron-beam irradiation [15].

6. Removal of NH_3

NH_3 is injected as an effective additive in the removal of SO_2 and NO_x . At the same time, NH_3 is not acceptable because it produce new environmental problem. To clearify the function of NH_3 in this process, the experiments of the removal of NH_3 are conducted in the flue gases with different conditions. The removal results are graphically presented in fig. 34. The figure shows that water content is the most important influence factor for NH_3 reduction. More than 85 % of 900 ppm NH_3 can be removed even without any electrical energy input at 21% H_2O content while less than 40 % of 720 ppm NH_3 is removed at 3 % H_2O content in the case of up to 8 Wh/Nm^3 energy input. As is well known, NH_3 is easily absorbed in water and , therefore, can be removed in the real flue gas. But removal of all NH_3 needs the electrical energy input, in particular, in the flue gas with low water content. In the flue gas with about 16 % H_2O, which is used in majority of our experiments, about 50 % of 900 ppm NH_3 can be removed as shown in fig.34. With corona discharge, NH_3 can partly be dissocited by corona discharge into variuos radicals such as NH, NH_2 ect. These radicals convert NO to N_2. In the process of SO_2 and NO_x removal, the formation of $(NH_4)_2SO_4$ and NH_4NO_3 through the chemical reactions play a important role for the reduction of NH_3 slip. These experimental results are in good agreement with [16].

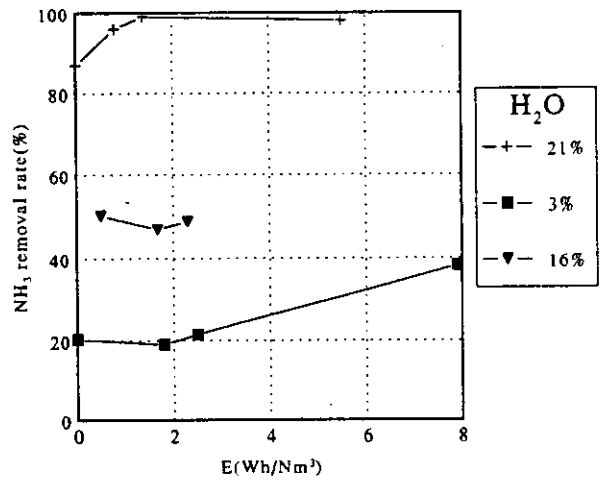

Figure 34: Removal of NH_3 in flue gases with different water.
(1:T=130 °C, t_{res}= 10 s, $[NH_3]_i$=900 ppm, O_2= 2.4%, CO_2= 10.5%, H_2O=21%;
2: T=70 °C, t_{res}= 6 s, $[NH_3]_i$=900 ppm, O_2= 6 %, CO_2= 8%, H_2O=16%;
3: T=90 °C, t_{res}= 10 s, $[NH_3]_i$=720 ppm, O_2= 18 %, CO_2= 1.5 %, H_2O=3%;).

7. Discussion

-dc bias level

In the experiments on the dc bias effect on the removal of NO and NO_x, it is found that the removal efficiency without dc bias is always better than that with dc bias. A use of dc bias being considered in general is to sweep the ions between two subsequent pulses in order to avoid the energy consumption on ions movement. At the first sight, the experimental results in fig.15 seem to be contrary to this idea. But, in fact, a residual voltage exits on the discharge gap after a pulse. This residual voltage is probably enough to sweep ions in the gap. With a additional dc bias, the more energy is input into the gas. But the conduction current after the streamer crosses the gap is increased with the development of the secondary streamer. The waveshape analysis indicates that with a use of dc bias, the current pulse and corresponding the power pulse become 50 ns wider. From this point of view, the energy is not used effectively with a dc bias, in particular, when dc bias is over the corona onset value.

-Chemistry process

In general, the plasma chemical process in the removal of SO_2 and NO from flue gas by pulsed corona discharge consists of three steps as follow:

1) When positive streamers propagate from anode to cathode with a characteristic velocity of 10^5-10^6 m/s, free electrons having a average energy of 10 eV are produced in the region of the front of the streamer head. Free electrons with such a energy can dissociate O_2, H_2O, N_2 and NH_3 to generate active radicals O, OH, H, and NH_2.

2) These active radicals initiate a large number of possible reactions to convert SO_2 into H_2SO_4 and NO into HNO_3, NO_2 and N_2 through oxidation and reduction process. The ions and molecules produced by electrons also play an important role in the process. In this stage, the reaction is called homogeneous.

3) When ammonia is injected, the sulphate acid and nitric acid are converted to solid salts. At the same time, the heterogeneous phase reaction occurs at the surface of these particles. Also the autothermal reactions develop even without any external discharge energy input.

The streamer propagation, production of electrons and subsequent radicals, gas-phase chemical reactions have been extensively investigated by experiments and model calculations. The main chemical paths are simply summarized in fig.35.

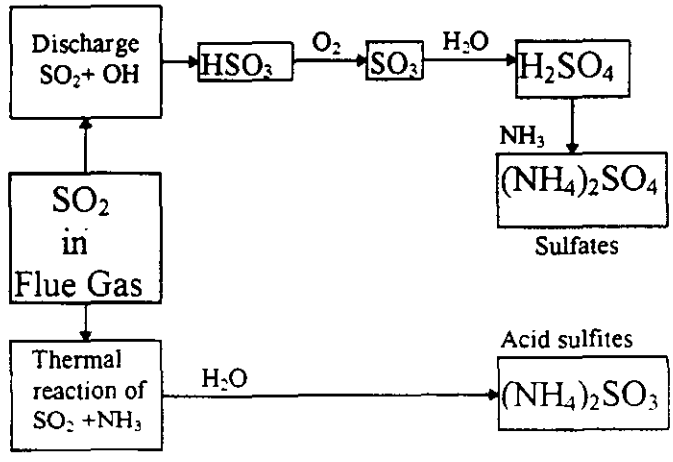

Fig. 35a: Reaction mechanism for removal of SO_2

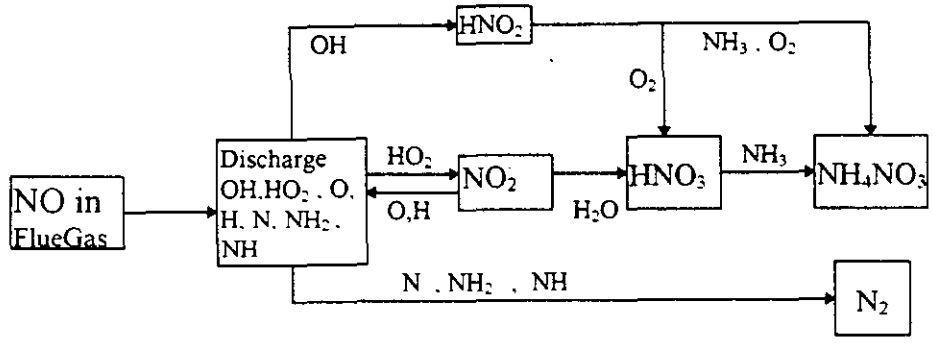

Fig. 35b: Reaction mechanism for removal of NO.

-SO_2 removal

For removal SO_2 without any additive use, OH, mainly produced by direct dissociation of H_2O and hydrated ions, is suggested as the most important radical. The main removal reactions are:

$SO_2 + OH \longrightarrow HSO_3$
$HSO_3 + O_2 \longrightarrow SO_3 + HO_2$
$SO_3 + H_2O \longrightarrow H_2SO_4$

The experimental results show that the removal of SO_2 by radical reaction is not very effective. Only less than 30 % of 300 ppm SO_2 is removed in the case of upto 10 Wh/Nm^3 energy input. The similar results are also obtained by using barrier discharge [17] and electron-beam irradiation [18]. The removal of SO_2 ultimately depends on the numer of OH radicals produced which in turn depends to a first order on power deposition. When NH_3 is injected, the removal of SO_2 is remarkably enhanced. In this case, the thermal reaction of SO_2-NH_3 leads to rather effective SO_2 removal. More energy input hardly improves the SO_2 conversion efficiency, but the slip NH_3 is significantly reduced. The by-product in this process is stable neutral sulphates $(NH_4)_2SO_4$ [3]. The thermal reaction of SO_2-NH_3 proceeds spontaneously and strongly depends on the gas temperature. By reducing the temperature, this thermal reaction is stronger. But the by-products are acid sulphates rather than neutral sulphates and therefore leads to much high leak NH_3. Acid sulphates can not be used as a fertiliser [3]. The apparent history effect in the removal of SO_2 with NH_3 injection is hard to explain with rapid gas-path reaction. The most likely explanation is the heterogeneous reaction because the aerosol formation and growth required longer time. The evidence of aerosol formation and enhancement on the removal of SO_2 is, however, still limited.

-Removal of NO and NO_x

The chemistry of the removal of NO and NO_x is much more complex than the removal of SO_2 in the discharge plasma. At EUT, a set of 1000 chemical kinetics equations was solved using the KINEL program. The most important reactions for the gas-path process are found as [4,10] :

$NO + OH \longrightarrow HNO_2$
$NO + HO_2 \longrightarrow NO_2 + OH$
$NO + N \longrightarrow N_2 + O$
$NO_2 + OH + M \longrightarrow HNO_3 + M$
$NO + O \longrightarrow NO_2$
$NO + O_3 \longrightarrow O_2 + NO_2$
$NO_2 + O \longrightarrow NO + O_2$
$NO_2 + H \longrightarrow NO + OH$

The reduction and oxidation reactions are both involved in the process. Without NH_3 injection, the NO removal mainly follows the oxidation path. The reverse reaction of NO_2 with O or H is a main obstacle in the way of the conversion of NO to H_2NO_3. Even when NO_2 reacts with H_2O, a NO molecule forms [4]:

$3NO_2 + H_2O \longrightarrow 2HNO_3 + NO$

So only two-thirds of the NO is eventually removed. The experimental result of a optimum residence time of 15 s is also evidence for this explanation. With NH_3 injection, there are two explanations for the

improvement of NO removal. The first is that the radicals NH_2 and NH produced by NH_3 dissociation react with NO [12]:

$NO+NH_2 \longrightarrow H_2O+N_2$
$NO+NH \longrightarrow N_2+OH$

The second is that HNO_3 is converted to NH_4NO_3. The general function of NH_3 can be thought that the formation of NO is inhibited by the presence of NH_3. With stoichiometric amount of NH_3, the high leak NH_3 indicates that the final products of NO conversion is not only NH_4NO_3 .

The presence of 300 ppm SO_2 can improve NO conversion a factor three in the case of no NH_3 injection. This effect is also strong for NO_x conversion. Though this fact is well known, the chemical mechanism is still unknown.

At EUT, the results of experiments and calculations have been put together. The calculated removal of NO molecules is still one to two order of amplitude lower than the value in reality. The most likely reason is that the heterogeneous reactions on the surface of aerosols and particles are not included in the model calculations.

-Combined removal of and NO

The importance of the heterogeneous reactions has been emphasized by the present experiments on combined removal of SO_2 and NO. As indicated in fig.31, a time-dependence of the removal of and NO with NH_3 injection is observed with a good reproducibility. The general tendency of the variation of NO concentration is quite similar to the variation of particle number as obtained in [18]. Concerning the strong synergetic effect between SO_2, NO and NH_3 on the removal of NO, the adjustment of the location of or NH_3 injection on the discharge reactor can enlarge this effect . The best results, i.e., 95 % and 85 % NO removal with 3 ppm leak NH_3 at 4 Wh/Nm^3 (13 eV/NO), are obtained under the considerations in several aspects:

1) The gas temperature is set at about 80 °C with 16% H_2O in the flue gas. The liquid-path reaction is possible to occur after the gas passed through the discharge reactor.

2) The optimum gas residence time of 15 s is used for this discharge reactor.

3) DC bias level is lower than its corona onset value.

4) SO_2 and NH_3 are injected at the different location of the reactor. The positive effect on the NO removal is effectively used.

5) Since the width of voltage and current pulses used in the experiments are three times larger than the streamer transit time of 30-40 ns, it could expected that the removal efficiency is further improved with shorter pulses[4].

-Two-stage treatment

The attempt to conduct two-stage treatment experiments is encouraged by the existing experiments with electron-beam irradiation. In the electron-beam irradiation treatment, the higher NO_x removal efficiency could be achieved in the double- and triple-stage irradiation compared to single-stage irradiation. The enhancement effect of the multi-stage irradiation is thought due to the conversion of some intermediate products such as nitrous acid (HNO_2) to stable forms during the irradiation pause in

between the multi-stage irradiation. In the single stage irradiation, the intermediate products will be decomposed through the reaction with OH radical to produce NO_x during the continuous irradiation [15]. This improvement does not appear in our experiments with pulsed corona discharge. This difference is probably ascribed to the difference between the two processes of the distribution of the electrons both in energy and space. In a streamer corona electrons are produced in thin discharge channels with a average energy of about 10 eV while in electron-beam irradiated gas the spatial distribution of electrons, with an energy of the order of 100 eV[20], is rather uniform. In a wire-cylinder discharge geometry the streamers fill only a small fraction of volume, i.e., 10^{-3}-10^{-4} [4]. The majority of the volume in the electrode gap is streamer free while a pulse is applied on the gap. On the other hand, the pulsed corona discharge is a process with a sequence of pauses. Therefore is not necessary to interrupt the discharge. In other words, in the pulsed corona discharge process, the double-stage treatment can not improve the cleaning efficiency .

8. Conclusions

1. UV absorption to simultaneously detect NO (0-450 ppm), SO_2 (0-1000 ppm) and NH_3 (0-1000 ppm) is applied to the flue gas cleaning process with pulsed corona discharge. The measurement error is in all cases below 5 % despite of spectral overlap. The good agreement on the removal effects with results from literature shows that this is a viable method.

2. DC bias increases the power input into the gas. But the cleaning efficiency for NO and NO_x becomes lower. This effect is stronger when the bias is above corona onset. The possible reason is that the pulses of current and power become wider and therefore the energy is not used effectively.

3. Considering the removal efficiency of NO_x and SO_2, the stability of by-products and the property of pulsed corona, optimum temperature is that just over water condensation;

4. The NO and NO_x removal requires the lowest power input at a residence time of about 15 s in this system. An optimum residence time for removal of NO/NO_x can be explained using reverse reactions. In the presence of SO_2 and NH_3, the reverse reactions of conversion of NO are likely to be inhibited, there is probabaly not such an optimum residence time.

5. The auto-thermal reaction of SO_2-NH_3 is dominant for SO_2 removal, but the slip NH_3 is high and the by-products are acid sulfite. The increase in input of discharge energy has only a small influence on the SO_2 removal, but the slip of NH_3 can be reduced to almost zero by increasing the power input. In combination of corona discharge and NH_3 injection, the by-products are sulfates which can be directly used as a fertilizer.

6. With corona discharges and NH_3 injection, it is found that the removal rates of SO_2 depend on the history of energizating the discharge, but hardly depend on the energy input. This history effect can improve the SO_2 removal rate by 20 %. In this process, NH_3 slip always depends on the energy input. This effect has not been explained well but it is supposed to relate to the formation of aerosols and/or salts.

7. NH_3 injection enhances the NO removal but its slip is high. The effect of NH_3 injection on the NO removal is thought to be due to the reduction of the formation of NO through the increase in the reduction reaction and nitric salts. The chemical mechanism in NO removal with NH_3 injection has, up to now, been unknown. Further investigations to expain high slip of NH_3 and low salts formation are needed.

8. 300 ppm SO_2 or 600 ppm NH_3 presence can enhance NO removal a factor three or two in 70 °C flue gas with 6 s residence time. However, in combination, the enhancement becomes less than either of them. The knowlege to explain this phenomenon can be a topic for the further study.

9. Synergetic effects on NO removal can be enlarged through adjusting locations of SO_2 or NH_3 injection. When 1200 ppm NH_3 is injected later, 81 % removal of 320 ppm NO (23 eV/NO) and over 98 % removal of 600 ppm SO_2 with less than 5 ppm leak NH_3 have been obtained at 7 Wh/Nm^3. In the case of 900 ppm NH_3 injection before the reactor and 300 ppm SO_2 injection later, 81 % removal of 320 ppm NO(25 eV/NO) and 97 % SO_2 removal are achieved with about 2 ppm NH_3 slip at 7.5 Wh/Nm^3. For the real flue gas, only the location adjustment for NH_3 injection is of practical importance.

10. The experiments on the removal of NO/NO_x and simultaneous removal of NO and SO_2 show that no improvement is given by using two-stage treatment instead of one-stage treatment. The results are quite different from the results obtained with electron-beam irradiation. This difference is probably ascribed to the difference of spatial and energy distribution of electrons between the two processes.

11. The best results, i.e. 95 % SO_2 and 85 % NO (about 13 eV/NO) removal with 3 ppm leak NH_3, are obtained at the conditions of 80 °C, 15 s residence time and 15 kV dc bias with synergetic and history effects.

12. With shorter pulses and no dc bias, 50 % improvement of NO removal efficiency is still expected. A suggestion for the further measurements is to evaluate the maximum cleaning efficiency using the conditions close to full optimization (temp.: around 70 °C, residence time: about 15 s, half-width of current pulses: 20-30 ns, dc bias: 0 kV, NH_3 injection : at half way of reactor, NO measurement: waiting for a stable concentration at the exit of system).

9 References

[1] Dinelli, G. and L. Civitano, M. Rea,
Industrial experiments on Pulse Corona simultaneous removal of NO_x and SO_x from flue gas.
IEEE Trans. on IAS, Vol. 26 (1990), No. 3, p. 535-41.

[2] Masuda, S.
Report on novel dry $DeNO_x/DeSO_x$ technology for cleaning combustion gases from utility thermal power plant boilers.
In: Penetrante, B. and S. Schultheis, eds. *Non-thermal plasmas for pollution control.*
Berlin: Springer, 1993. NATO ASI Series, Vol. G 34B. P. 131-138.

[3] Civitano, L.
Industrial application of corona processing to flue gas.
In: Penetrante, B. and S. Schultheis, eds. *Non-thermal plasmas for pollution control.*
Berlin: Springer, 1993. NATO ASI Series, Vol. G 34B. P. 103-130.

[4] Veldhuizen, E.M.van and W.R.Rutgers, V.A.Bityurin
Energy efficiency of NO removal by pulsed corona discharges.
Plasma Chemistry and Plasma Processing,Vol. 16 (1996), No. 2, p. 227-247.

[5] Veldhuizen, E.M.van and L.M.Zhou, A.H.F.M.Baede, and W.R.Rutgers
UV absorption to determine SO_2, NO and NH_3 in flue gas cleaning by pulsed corona.
In: Proc. HAKONE V Conference, Brno, 1-4 Sept. 1996. Ed. By Drimal, J. Brno: Masaryk University, 1996. P. 107-111.

[6] Veldhuizen, E. M. van and L.M.Zhou, W.R. Rutgers
Synergetic effects in the pulsed corona SO_2/NO_x conversion from flue gas.
In: Proc. 3rd Int. Seminar on Nonequilibrium processes and their appl., Minsk, 8-13 Sept. 1996. Ed. By Zhdanok, S.A. Minsk: A.V. Luikov Heat and Mass Transfer Institute, 1996. P. 14-18.

[7] Creyghton, Y. L. M. and W.R.Rutgers, E.M. van Veldhuizen
In-situ investigation of pulsed corona discharge.
Eindhoven: Eindhoven Univ. of Technology, Faculty of Electrical Eng., 1993. EUT Report 93-E-279.

[8] Creyghton, Y.L.M. and E.M.van Veldhuizen, W.R.Rutgers
Diagnostic techniques for atmospheric streamer discharges.
IEE Proc.-Sci. Meas. Technol.,Vol. 141 (1994), No. 2, p. 141-152.

[9] Belousova, E.V. e.a.
Removal of SO_2,NO_x and organic impurities from atmospheric air by simultaneous exposure to pulsed and dc corona discharge.
Khim. Vys. Energ. (Eng. transl.),Vol. 25 (1992), p. 468-469.

[10] Veldhuizen, E.M.van and M. A. Tas, W.R. Rutgers
Measured and calculated NO removal by pulsed corona.
In: Proc. Int. Workshop on Plasma Technologies for Pollution Control and Waste Treatment,

Beijing, 10-14 May 1996. Ed. by Li, R. Beijing Institute of Technology, 1996. P. 57-66.

[11] Tas, M.A.
Plasma-induced catalysis: a feasibility study and fundamentals.
PhD thesis, Eindhoven University of Technology, The Netherlands, 1995.

[12] Chang, J.S. et al.
Preliminary pilot plant tests of a corona discharge-electron beam hybrid combustion flue gas cleaning system.
IEEE Trans. on IAS, Vol. 32 (1996), No. 2, p. 131-137.

[13] Li, R. and K.Yan, Y. Pu, E. Sani, F. Mattachini, M. Rea, E.M. van Veldhuizen
Removal of SO_2 by pulsed corona streamer.
In: Proc. American-China Workshop on Pollutants Control, Beijing, 20-25 July, 1995. Ed. by Li, R. Beijing: Beijing Institute of Technology, 1996.

[14] Niessen, W. and M. Neiger, R. Schrufts
Modelling of the removal of nitric monoxide from exhausts by dielectric barrier discharges.
In: Proc. ISPC-12, Minneapolis, Minnesota, USA, 21-25 August, 1995. Ed. By Heberlein, J.V. and D.W. Ernie, J.T. Roberts. Minneapolis: University of Minnesota, 1995. P. 667-682.

[15] Maezawa, A. and M. Izutsu
Application of E-beam treatment to flue gas cleaning in Japan.
In: Penetrante, B. and S. Schultheis, eds. *Non-thermal plasmas for pollution control.*
Berlin: Springer, 1993. NATO ASI Series, Vol. G 34B. P.47-54.

[16] Chakrabarti, A. et al.
Gas cleaning with semi-wet type plasma reactor.
IEEE Trans. on Ind. Appl. Vol. 31 (1995), No. 3, p. 500-506.

[17] Chang, M.B. and M.J. Kushner, M. J. Rood
Removal of SO_2 and the simultaneous removal of SO_2 and NO from simulated flue gas streamers using the dielectric barrier discharge plasmas.
Plasma Chemistry and Plasma Processing, Vol. 2 (1993), No. 4, p. 565-580.

[18] Frank, N.W. and S. Hirano
The history of electron beam processing for enviromental pollution control and work performed in the United States.
In: Penetrante, B. and S. Schultheis, eds. *Non-thermal plasmas for pollution control.*
Berlin: Springer, 1993. NATO ASI Series, Vol. G 34A. P1-26.

[19] Christensen, P.S.
The formation of areosols from SO_2 and NH_3 in humid air.
PhD thesis, Technical University of Denmark, 1994.

[20] Creyghton, Y.L.M.
Pulsed positive corona discharges: fundamental study and application to flue gas treatment.
PhD thesis, Eindhoven University of Technology, The Netherlands, 1993.

Eindhoven University of Technology Research Reports ISSN 0167-9708
Coden: TEUEDE

Faculty of Electrical Engineering

(277) Weiland, Siep
A BEHAVIORAL APPROACH TO BALANCED REPRESENTATIONS OF DYNAMICAL SYSTEMS.
EUT Report 93-E-277. 1993. ISBN 90-6144-277-X

(278) Gorshkov, Yu.A. and V.I. Vladimirov
LINE REVERSAL GAS FLOW TEMPERATURE MEASUREMENTS: Evaluations of the optical arrangements for the instrument.
EUT Report 93-E-278. 1993. ISBN 90-6144-278-8

(279) Creyghton, Y.L.M. and W.R. Rutgers, E.M. van Veldhuizen
IN-SITU INVESTIGATION OF PULSED CORONA DISCHARGE.
EUT Report 93-E-279. 1993. ISBN 90-6144-279-6

(280) Li, H.Q. and R.P.P. Smeets
GAP-LENGTH DEPENDENT PHENOMENA OF HIGH-FREQUENCY VACUUM ARCS.
EUT Report 93-E-280. 1993. ISBN 90-6144-280-X

(281) Di, Chennian and Jochen A.G. Jess
ON THE DEVELOPMENT OF A FAST AND ACCURATE BRIDGING FAULT SIMULATOR.
EUT Report 94-E-281. 1994. ISBN 90-6144-281-8

(282) Falkus, H.M. and A.A.H. Damen
MULTIVARIABLE H-INFINITY CONTROL DESIGN TOOLBOX: User manual.
EUT Report 94-E-282. 1994. ISBN 90-6144-282-6

(283) Meng, X.Z. and J.G.J. Sloot
THERMAL BUCKLING BEHAVIOUR OF FUSE WIRES.
EUT Report 94-E-283. 1994. ISBN 90-6144-283-4

(284) Rangelrooij, A. van and J.P.M. Voeten
CCSTOOL2: An expansion, minimization, and verification tool for finite state CCS descriptions.
EUT Report 94-E-284. 1994. ISBN 90-6144-284-2

(285) Roer, Th.G. van de
MODELING OF DOUBLE BARRIER RESONANT TUNNELING DIODES: D.C. and noise model.
EUT Report 95-E-285. 1995. ISBN 90-6144-285-0

(286) Dolmans, G.
ELECTROMAGNETIC FIELDS INSIDE A LARGE ROOM WITH PERFECTLY CONDUCTING WALLS.
EUT Report 95-E-286. 1995. ISBN 90-6144-286-9

(287) Liao, Boshu and P. Massee
RELIABILITY ANALYSIS OF AUXILIARY ELECTRICAL SYSTEMS AND GENERATING UNITS.
EUT Report 95-E-287. 1995. ISBN 90-6144-287-7

(288) Weiland, Siep and Anton A. Stoorvogel
OPTIMAL HANKEL NORM IDENTIFICATION OF DYNAMICAL SYSTEMS.
EUT Report 95-E-288. 1995. ISBN 90-6144-288-5

(289) Konieczny, Pawel A. and Lech Józwiak
MINIMAL INPUT SUPPORT PROBLEM AND ALGORITHMS TO SOLVE IT.
EUT Report 95-E-289. 1995. ISBN 90-6144-289-3

(290) Voeten, J.P.M.
POOSL: An object-oriented specification language for the analysis and design of hardware/software systems.
EUT Report 95-E-290. 1995. ISBN 90-6144-290-7

Eindhoven University of Technology Research Reports ISSN 0167-9708
Coden: TEUEDE

Faculty of Electrical Engineering

(291) Smeets, B.H.T. and M.H.J. Bollen
STOCHASTIC MODELLING OF PROTECTION SYSTEMS: Comparison of four mathematical techniques.
EUT Report 95-E-291. 1995. ISBN 90-6144-291-5

(292) Voeten, J.P.M. and A. van Rangelrooij
CCS AND TIME: A practical and comprehensible approach to a performance evaluation of finite state CCS descriptions.
EUT Report 95-E-292. 1995. ISBN 90-6144-292-3

(293) Voeten, J.P.M.
SEMANTICS OF POOSL: An object-oriented specification language for the analysis and design of hardware/software systems.
EUT Report 95-E-293. 1995. ISBN 90-6144-293-1

(294) Osch, A.W.H. van
MODELLING OF PRASEODYMIUM-DOPED FLUORIDE AND SULFIDE FIBRE AMPLIFIERS FOR THE 1.3 μM WAVELENGTH REGION.
EUT Report 95-E-294. 1995. ISBN 90-6144-294-X

(295) Bastiaans, Martin J.
GABOR'S EXPANSION AND THE ZAK TRANSFORM FOR CONTINUOUS-TIME AND DISCRETE-TIME SIGNALS: Critical sampling and rational oversampling.
EUT Report 95-E-295. 1995. ISBN 90-6144-295-8

(296) Blaschke, F. and A.J.A. Vandenput
REGELTECHNIEKEN VOOR DRAAIVELDMACHINES. (Control of AC machines, in Dutch)
2 Volumes. Vol. 1: TEKST (Text). Vol. 2: FIGUREN (Figures).
EUT Report 96-E-296. 1996. ISBN 90-6144-296-6

(297) Dolmans, G.
DIVERSITY SYSTEMS FOR MOBILE COMMUNICATION IN A LARGE ROOM.
EUT Report 96-E-297. 1996. ISBN 90-6144-297-4

(298) Mazák, J. and J.L.F. Balseiro
MODELING OF A FLUIDIZED BED REACTOR FOR ETHYLENE POLYMERIZATION.
EUT Report 96-E-298. 1996. ISBN 90-6144-298-2

(299) Butterweck, H.J.
ITERATIVE ANALYSIS OF THE STEADY-STATE WEIGHT FLUCTUATIONS IN LMS-TYPE ADAPTIVE FILTERS.
EUT Report 96-E-299. 1996. ISBN 90-6144-299-0

(300) Horck, F.B.M. van and A.P.J. van Deursen, P.C.T. van der Laan
COUPLING ON A MULTILAYER PRINTED CIRCUIT BOARD AND THE CURRENT DISTRIBUTION IN THE GROUND PLANE.
EUT Report 96-E-300. 1996. ISBN 90-6144-300-8

(301) Veen, J.L.F. van der and L.J.J. Offringa
ROTOR LOSSES IN A HIGH SPEED SYNCHRONOUS GENERATOR WITH PERMANENT MAGNET EXCITATION AND RECTIFIER LOAD.
EUT Report 96-E-301. 1996. ISBN 90-6144-301-6

(302) Zhou, L.M. and E.M. van Veldhuizen
MEDIUM-SCALE EXPERIMENTS ON DeNO/DeSO2 FROM FLUE GAS BY PULSED CORONA DISCHARGE.
EUT Report 96-E-302. 1996. ISBN 90-6144-302-4